Mapping mining-affected water pollution in China: Status, patterns, risks, and implications

Ziyue Yin[1], Jian Song[2], Dianguang Liu[1], Jianfeng Wu[1,*], Yun Yang[2], Yuanyuan Sun[1], Jichun Wu[1]

[1] Key Laboratory of Surficial Geochemistry, Ministry of Education, Department of Hydrosciences, School of Earth Sciences and Engineering, Nanjing University, Nanjing 210023, China

[2] School of Earth Sciences and Engineering, Hohai University, Nanjing 211100, China

[*] Corresponding authors. Tel: +86 25 89680853; fax: +86 25 83686016

E-mail address: jfwu@nju.edu.cn (J.F. Wu)

Abstract: Mining-affected water pollution poses a serious threat to human health and economic prosperity globally. The human toxicity and ecosystem impacts induced by mining activities have achieved considerable public, scientific, and regulatory attention. In this study, a comprehensive database of 8,433 water samples from 211 coal mines and 87 metal mines in China was established to reveal the national status and spatial heterogeneity of mining-affected water pollution, human health risks, and their potential multifaceted challenges. The results show that the concentrations of sulfate, Fe, Mn, Al, and several heavy metals in the mining-affected water of metal mines are generally higher than those of coal mines, especially in acid water (pH < 6.5). In terms of spatial distribution, the gridded data demonstrates that the southern regions in China, especially Guizhou, Guangdong, Fujian, Jiangxi, Hunan, and Guangxi provinces/autonomous regions, are the hotspots of mining-affected water pollution (*i.e.*, low pH as well as high sulfate, Fe, Mn, and heavy metals). The risk assessment reveals that t~~T~~he unacceptable carcinogenic risks caused by poor-quality surface water and groundwater are observed in 51.52% (for adults) and 29.29% (for children) of the mining areas. Moreover, severe non-carcinogenic risks are also identified in 68.07% and 80.67% of mining areas for adults and children, respectively. Overall, the acid and metal-rich water exhibits a widespread and detrimental impact in China, especially in the southern regions, posing significant risks to planetary health by degrading surface water and groundwater quality, destroying biodiversity, and threatening human well-being. This study provides a thorough set of scientific data on surface water and groundwater quality in mining areas to guide policymakers in designing differentiated management strategies for the sustainable development of coal and metal mines.

Keywords: Mining-affected water pollution; Spatial patterns; Risk assessment; Adverse effects; Differentiated management.

1 Introduction

Coal and metalliferous mineral resources are essential materials for global socio-economic development. The extraction and processing of minerals have caused detrimental impacts on aquatic ecosystems, soil ecosystems, living organisms, and human health worldwide (Blowes et al., 2014; Li et al., 2014; Havig et al., 2017; Ighalo et al., 2022). Mine drainage and leachate from active and abandoned mines are of global concern as they continue to release harmful substances into the underlying geological materials or adjacent water bodies for decades, inevitably leading to the degradation of both surface water and groundwater quality (Acharya and Kharel, 2020; Ighalo and Adeniyi, 2020). In particular, the environmental risks induced by acid mine drainage (AMD) have been ranked second only to global warming and ozone depletion (Moodley et al., 2018; Ai et al., 2023). Mining-affected water is generally characterized as metalliferous. Certain metals, such as Cu, Fe, Mn, and Zn, function as essential trace elements in human physiological processes. However, when their concentrations exceed specific thresholds in surface water and groundwater systems, these biologically relevant metals can pose significant toxicological risks to ecosystems and human health (Wei et al., 2022). Other non-essential heavy metals (HMs), including As, Cd, Cr, Hg, Ni, and Pb, have no nutritional or beneficial effects on humans. They can be toxic even at low concentrations and are therefore recognized as carcinogenic, mutagenic, and teratogenic. In addition, the persistence, toxicity, mobility, and non-biodegradability of HMs potentially form an enduring environmental footprint that jeopardizes ecosystems (He et al., 2013; Dippong et al., 2024). Consequently, there is a growing demand in mining areas for assessing the status of pollution and associated risks, as well as developing more effective management strategies and policies to mitigate these detrimental impacts (Cheng 2003; Hu et al., 2014).

Exploring the heterogeneity, risks, and threats of mining-affected water pollution is desirable but remains challenging. More recently, an increasing number of studies have been focused on the mining-affected water pollution from coal mines in major coal-producing countries (Sun et al., 2013; 2020; 2025; Acharya and Kharel, 2020; Dong et al., 2022; Ai et al., 2023; Hou et al., 2024; Kumar et al., 2024). For instance, Acharya and Kharel (2020) provided an in-depth overview of the formation and effects of AMD from coal mining in the United States, reviewed prediction and treatment methods, identified key research gaps, and explored the challenges and opportunities that AMD posed for scientists and researchers. Ai et al. (2023) developed a conceptual model to illustrate the formation and evolution of AMD in the coal mines from a life-cycle perspective. Meanwhile, the critical governing factors and treatment technologies of AMD across abandoned mines in major coal-producing countries were identified, including China, the United States, the United Kingdom, Australia, and India. Coal and metal mines have different priority pollutants and levels of pollution due to differences in geological conditions and mineral extraction methods (Yu et al., 2024). Comparative studies of the status, heterogeneity, risks, and impacts of water pollution in coal and metal mines achieved limited concerns so far. It is essential for the development of remediation strategies and the implementation of risk-based, differentiated management practices to achieve sustainability in mining areas associated with the mineral economy.

To our knowledge, previous studies have provided a solid basis for the soil pollution status of HMs and their related health risk at the national or global scale (Li et al., 2014; Liu et al., 2020; Hou et al., 2023; Shi et al., 2023). For example, Shi et al. (2023) identified the spatiotemporal distribution of soil HM concentrations based on studies conducted between 1977 and 2020. In addition, the ecological and human health risks were assessed concerning different land use types

at the national scale. Yu et al. (2024) provided a more comprehensive analysis of the pollution characteristics, spatial distribution, major influencing factors, and probabilistic health risks of potentially toxic elements in soil, using data from 110 coal mines and 168 metal mines across China. However, systematic studies of water pollution status and risks have yet to be undertaken at a national or even broader scale, as current research only focused on water pollution and risks in specific mining areas (He et al., 1998; Xiao et al., 2003; Wang et al., 2019; Chen et al., 2020; Wang et al., 2023). Therefore, it is necessary to implement deep mining of massive hydrochemical data and establish a nationwide database that can identify the spatial pattern of mining-affected water pollution and support risk assessment.

China, the second-largest economy worldwide, has various and extensive mineral resources (Li et al., 2014). It has been demonstrated that there are 171 types of mineral resources in China, with proven reserves accounting for 12% of the world's mineral resources (Hu et al., 2009). Furthermore, China is one of the largest global producers and consumers of metals and metalloids, such as Fe, Mn, Zn, Pb, Sb, and Sn (Gunson and Jian, 2001). China's coal reserves of 143,197 million tons (Mt) rank fourth globally, while its annual production of 2,971 Mt leads worldwide (Blowes et al., 2014; Ai et al., 2023). The coal extraction inevitably generates substantial amounts of mine water, resulting in a series of water environmental issues (Zhang et al., 2016b; Qu et al., 2023). For example, Gu et al. (2021) demonstrated a 2:1 mine water to coal production ratio, with approximately 2 tons of mine water produced per ton of extracted coal in China. In recent years, China has put forward a series of monitoring, prevention, management, and remediation measures to improve water quality and ensure water supply safety. However, the detrimental impacts triggered by mining activities on the aquatic environment have not been well managed. Since 2010,

China has implemented a policy-driven initiative to phase out nearly 12,000 coal mines to address two critical challenges, *i.e.*, the declining economic viability and the escalating environmental externalities (Ma et al., 2020). These policies effectively restore water storage capacity in mining regions. However, sulfates and dissolved metals generated by complex geochemical processes during the weathering of sulfide minerals may migrate and transform within the recovering groundwater system, thereby increasing the ecological vulnerability of local hydrological networks.

Therefore, the objectives of the study are: (i) to establish a national-scale high-quality database containing basic water quality information for typical coal and metal mines; (ii) to reveal spatial heterogeneity of mining-affected water and evaluate health risks posed by potentially toxic elements from coal and metal mines drainage in China; and (iii) to highlight the negative impacts and discuss the management implications in the differentiated policy for different mine types (coal or metal) and multiple mining phases (active or abandoned). Exploring the spatial heterogeneity of mining-affected water in China is of great importance to achieve deep insights for designing the targeted and promising mitigation strategies at the different spatial scales, which is critical to implementing the optimal trade-offs between green mining and human health.

2 Data and methodology

2.1 Data mining and processing

The belief information of natural resources in China has been presented in Section S1 of the Supplement, which serves as the cornerstone for the database development, spatial pattern analysis, and risk assessment in the study. Specifically, Figs. S1 and S2 illustrate the spatial distribution and total sulfur content of coal-bearing areas in China, and Fig. S3 exhibits the spatial distribution of

the major non-ferrous mineral resources in China. In this study, the composite database integrates mining-affected water (surface water and groundwater) quality parameters systematically extracted from 293 peer-reviewed studies published over the past decades. The primary data were obtained from mainstream online bibliographic databases, such as China National Knowledge Infrastructure, China Wanfang Literature Database, Web of Science, Elsevier, Springer, Wiley, Taylor & Francis, and the Multidisciplinary Digital Publishing Institute. The screening keywords were 'China', 'coal mine', 'metal mine', 'acid mine drainage', 'mine water', 'surface water', 'groundwater', 'hydrochemistry', and 'heavy metals'. All retrieved literature was downloaded by 2024/4/25, and the irrelevant studies were eliminated based on their abstracts, data, and full-text content.

2.2 Quality assessment

To ensure the reliability of the data, the collected literature was assessed for quality based on the following criteria: (i) adhering to strict quality assurance/quality control procedures during sampling, storage, and laboratory testing to ensure consistency, precision, and accuracy of results; (ii) extracting the sampling year (if not stated, the received or published date of the manuscript was adopted); (iii) extracting the latitude and longitude coordinates of the sampling site, mine or the county-level city in which they are located; and (iv) extracting the concentration of the featured component or statistics (minimum, mean and maximum value) based on the original data.

2.3 Database establishment

To assess the national extent of mining-affected water pollution, a comprehensive database of 8,433 data (6,175 coal mine data and 2,258 metal mine data) derived from 298 mines was established, including 211 coal mines and 87 metal mines (*i.e.*, antimony mine, copper mine, gold

mine, hematite mine, iron mine, lead-zinc mine, molybdenum mine, polymetallic mine, pyrite mine, rare earth mine, thallium-mercury mine, tin mine, tungsten mine, and uranium mine). The spatial distribution of the sampling site used in the study and the data classification at the provincial level are displayed in Fig. 1. The detailed information includes the sample ID, province, county/mine name, latitude (N), longitude (E), mine type, mine status (active or abandoned), sampling year, sampling month, sample type, basic physiochemical characteristics (pH, temperature (T), electrical conductivity (EC), oxidation reduction potential (ORP), dissolved oxygen (DO), and total dissolved solids (TDS)), major cation/anion ions (Na^+, K^+, Ca^{2+}, Mg^{2+}, Cl^-, SO_4^{2-}, HCO_3^-, NO_3^- and F^-), Fe, Mn, Al, HMs (Cr, Ni, Cu, Zn, As, Cd, Hg, and Pb) and data source. The typical mine lists used in the study are shown in Table S1.

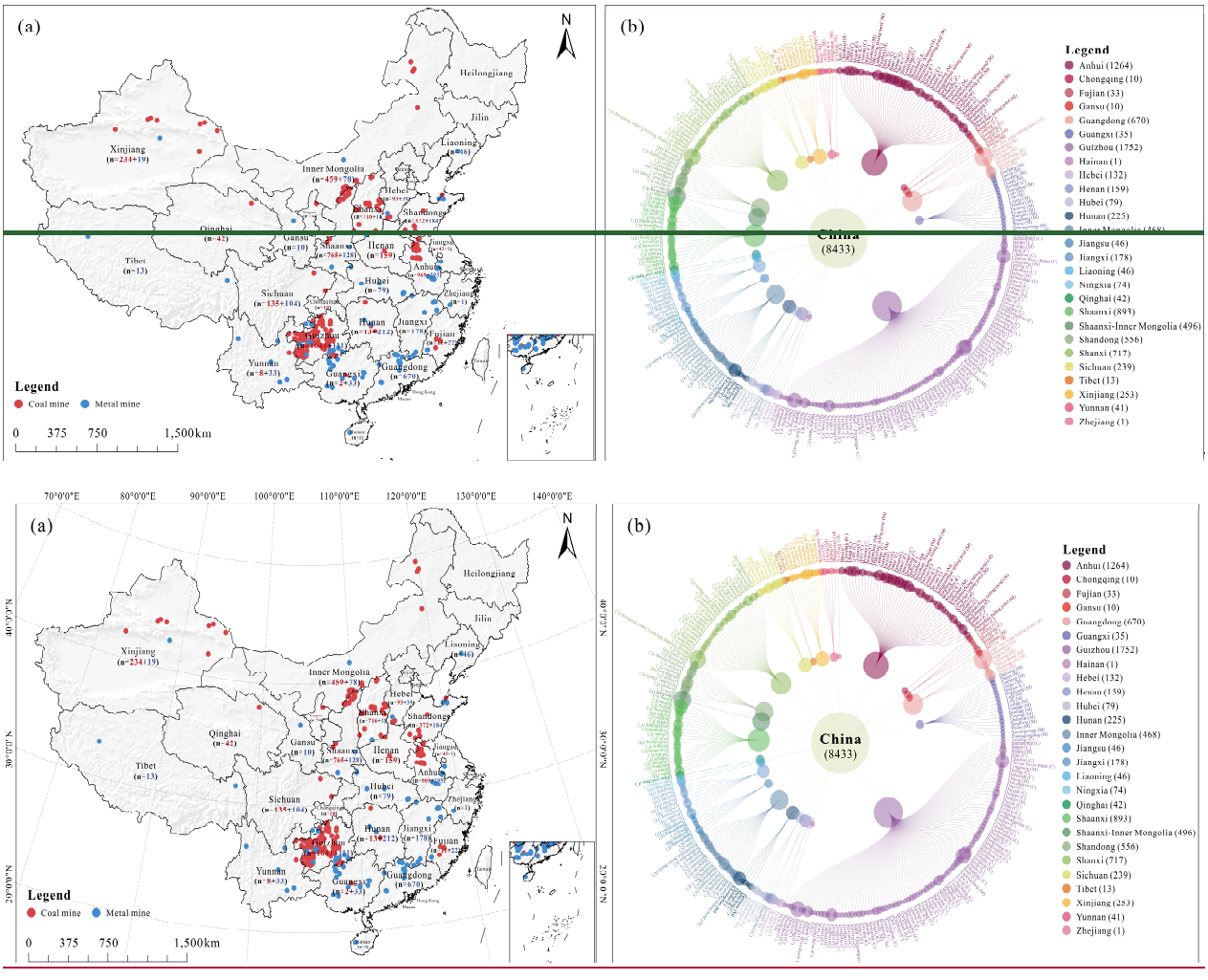

Figure 1. The information on data sources for this study, including (a) the spatial distribution of the sampling site, and (b) the data classification at the provincial level. In Fig. 1a, the value in the bracket represents the sample size (n), specially, the red and blue numbers are the sample sizes of coal mines and metal mines for different provinces, respectively. In Fig. 1b, the size of the inner circle represents the sample size at the provincial level, while the size of the outer circle represents the sample size at the specific mine level (the letters 'C' and 'M' in the brackets represent coal mine and metal mine, respectively). In the legend, the value in the bracket represents the sample size of the different provinces.

2.4 Risk assessment

Human exposure to metals can occur through various pathways, including ingestion and dermal contact with contaminated water. Therefore, these two pathways are considered to assess the potential human risks, *i.e.*, non-carcinogenic risks (NCRs) and carcinogenic risks (CRs), for adults and children. The model developed by the U.S. Environmental Protection Agency (US EPA) is employed for risk assessment in this study (US EPA, 2004; 2011):

$$ADI_{ing} = \frac{C_w \times IR \times EF \times ED}{BW \times AT} \quad (1)$$

$$ADI_{der} = \frac{C_w \times K_p \times ET \times SA \times EF \times ED \times CF}{BW \times AT} \quad (2)$$

where ADI_{ing} and ADI_{der} are the average daily intake by ingestion and dermal adsorption (mg/kg·d), respectively; C_w is the metal concentration in the mining-affected water (mg/L); IR is the ingestion rate (L/d); EF is the exposure frequency (d/yr); ED is the exposure duration (yr); K_p is the permeability coefficient of skin (cm/h); ET is the exposure time (h/d); SA is the exposed skin surface area (cm^2); CF is the conversion factor (L/cm^3), which is set to 0.001 in the study; BW is

the body weight (kg); and AT is the averaging time (d).

The hazard quotient (HQ) and hazard index (HI) are used to determine the NCRs to human health (Dippong et al., 2024). The HQ to residents (adults and children) from metal exposure via ingestion (HQ_{ing}) and dermal absorption (HQ_{der}) are quantified:

$$HQ_{ing} = \frac{ADI_{ing}}{RfD_o} \quad \text{and} \quad HQ_{der} = \frac{ADI_{der}}{RfD_{der}} \tag{3}$$

$$HI = \sum HQ_i = HQ_{ing} + HQ_{der} \tag{4}$$

where HI is the hazard index, which is the sum of HQ. HI > 1 indicates potential adverse effects on human health, whereas HI < 1 suggests no NCR is present; RfD_o is the reference dose for oral intake; and RfD_{der} is the reference dose for dermal exposure, which can be calculated by:

$$RfD_{der} = RfD_o \times ABS_{GI} \tag{5}$$

where ABS_{GI} is the gastrointestinal digestion coefficient (unitless).

The CRs to residents from ingestion and dermal absorption of mining-affected water are determined using Eqs. (6) and (7):

$$CR_{ing} = ADI_{ing} \times SF \quad \text{and} \quad CR_{der} = ADI_{der} \times SF \tag{6}$$

$$TCR = \sum CR_i = CR_{ing} + CR_{der} \tag{7}$$

where TCR is the total CR, if TCR > 10^{-4}, there is a significant risk to humans, and if $10^{-6} \leq$ TCR $\leq 10^{-4}$, the risk is generally acceptable; CR_{ing} and CR_{der} are the CRs induced by ingestion and dermal contact with mining-affected water, respectively; SF is the slope factor. The detailed values of the parameters in the above formula (Eqs. (1) - (7)) are represented in Tables S2 and S3.

3 Results and analysis

3.1 Overview of mining-affected water in China

All the data were collected from 26 provinces in China, while Beijing, Tianjin, Shanghai, Heilongjiang, Jilin, Hong Kong, Macao, and Taiwan did not meet the data extraction principles. At the provincial administrative level, five regions (*i.e.*, Guizhou, Anhui, Shaanxi, Shanxi, and Guangdong) have a statistically significant representation in sample collection. Among these, Guizhou and Anhui exhibit the most substantial data size, accounting for 20.78% and 14.99% of the total national dataset, respectively (Fig. 1). The spatial distribution of the sample size for each component at the 0.5° grid scale is depicted in Fig. S4. In general, most of the data show the basic information of the water sample, such as pH value and the concentrations of major cation and anion ions. In addition, many studies focused on the status of HM pollution in the mining areas, with a multi-source research synthesis revealing substantial monitoring coverage of 2,241 (Fe), 2,265 (Mn), 1,401 (Al), 952 (Cr), 691 (Ni), 1,563 (Cu), 1,575 (Zn), 1,451 (As), 1,627 (Cd), 280 (Hg), and 1,425 (Pb) water samples nationwide. Therefore, the Fe, Mn, Cd, Cu, and Zn are priority investigative targets for mine water research. The statistics of acid and neutral/alkaline mining-affected water in China are presented in Table 1. The pH and multi-component concentrations of mining-affected water in China are shown in Fig. 2.

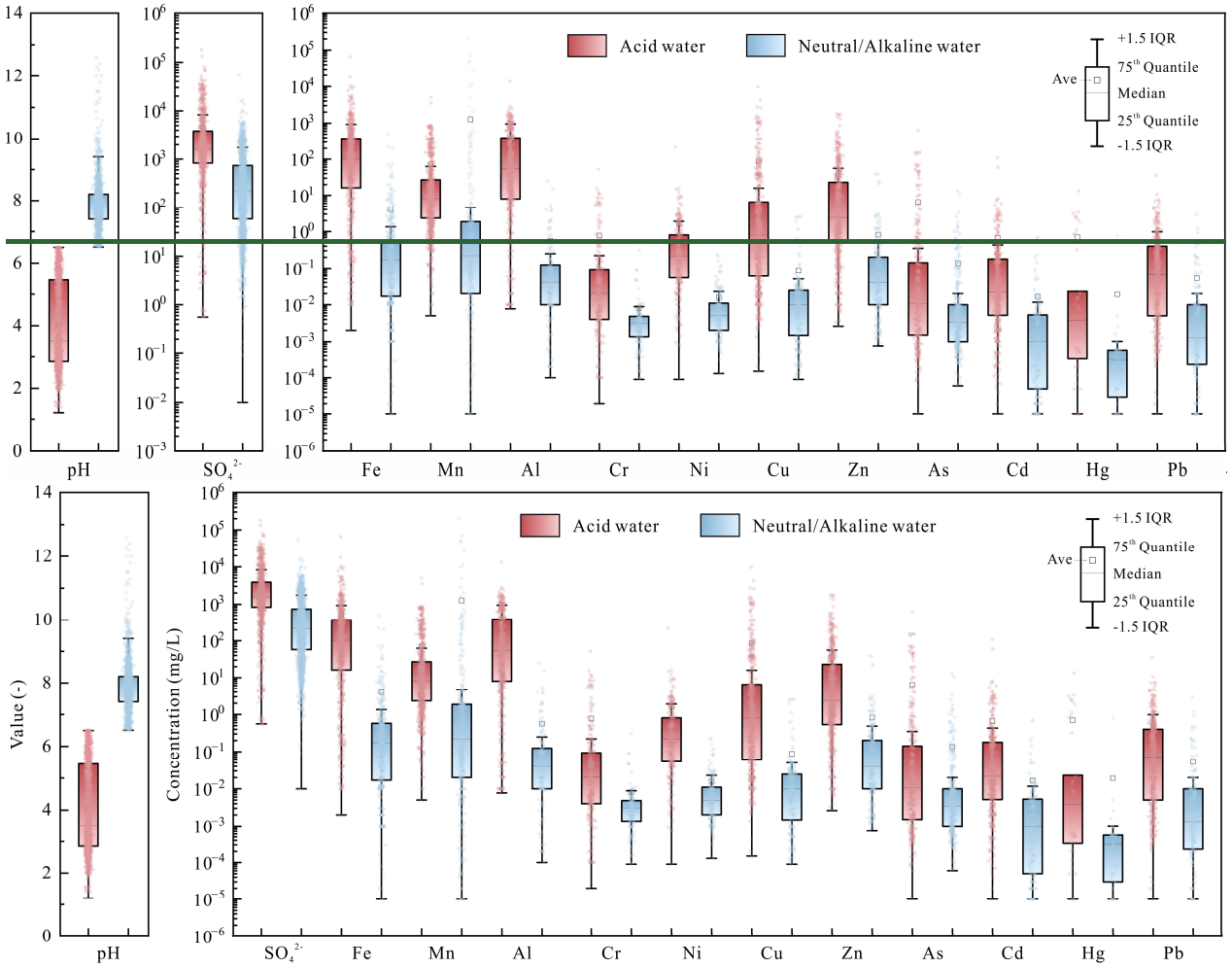

Figure 2. ~~Boxplots of the pH and multi-component concentrations (mg/L) of mining-affected water in China~~Statistical summary (minimum, median, average, and maximum) of the main species aggregated from all samples measured in mining-affected water in China (Units are mg/L except pH).

Table 1. Statistical summary (minimum, median, average, and maximum) of the main species aggregated from all samples measured in acid or non-acid mining-affected water in China (Units are mg/L except pH)~~The statistics of mining-affected water in China (Units are mg/L except pH)~~.

Item	Acid mining-affected water				Non-acid mining-affected water			
	Min	Median	Ave	Max	Min	Median	Ave	Max
pH	1.20	3.52	4.04	6.50	6.51	7.80	7.85	12.60
Na^+	0.00	15.60	55.39	1613	0.23	156.01	403.20	9371
K^+	0.00	3.30	6.41	172.00	0.00	3.11	7.10	419.00
Ca^{2+}	0.83	284.80	284.33	987.97	0.00	64.10	119.76	4841.70
Mg^{2+}	0.01	75.33	388.36	10992	0.00	19.01	52.85	12752
Cl^-	0.00	3.50	35.50	3097.40	0.00	51.68	314.21	26265
SO_4^{2-}	0.56	1580.16	4648.54	181000	0.01	181.27	621.24	52915
HCO_3^-	0.00	1.89	48.65	769.00	0.00	253.23	343.13	4976.61
NO_3^-	0.00	0.80	16.46	735.60	0.00	3.78	16.02	1774.95
F^-	0.00	0.69	4.17	238.34	0.00	0.81	1.91	100.00
Fe	0.0020	103.30	520.44	65250	0.00	0.1700	3.98	495.43
Mn	0.0050	8.11	71.18	5050	0.00	0.2164	1258.99	200000
Al	0.0077	53.90	304.92	13679	0.0001	0.0350	0.53	25.00
Cr	0.0000	0.0200	0.77	52.27	0.0001	0.0031	0.01	0.31
Ni	0.0001	0.2166	1.64	216.00	0.0001	0.0050	0.02	0.23
Cu	0.0002	0.8010	85.64	9777.77	0.0001	0.0100	0.07	2.56
Zn	0.0026	2.3685	46.63	1834	0.0007	0.0391	0.53	39.30
As	0.00	0.0108	6.50	641.70	0.0001	0.0034	0.14	13.00
Cd	0.00	0.0220	0.66	110.00	0.00	0.0004	0.01	0.67
Hg	0.00	0.0038	0.70	13.36	0.00	0.0003	0.02	0.78
Pb	0.00	0.0700	0.51	35.68	0.00	0.0012	0.03	1.22

It should be highlighted that the mean values may result in overestimation, as some extremely high values are observed in the surveyed mines, such as the Baiyin copper mine, Bainiuchang polymetallic mine, Zijinshan copper mine, and so on. Therefore, median values are selected to represent the national characteristics of the mining-affected water pollution in this section. The pH value of acid water (*i.e.*, pH < 6.5) ranges from 1.20 to 6.50, with a median (interquartile range, IQR) of 3.52 (2.85, 5.45) (CV = 34.39%). In comparison, neutral/alkaline water has a pH value between 6.51 and 12.60, with a median of 7.80 (IQR: 7.40, 8.20) (CV = 8.99%). Generally, the SO_4^{2-} concentration of acid water is higher than that of neutral/alkaline water (Figs. 2 and 3). The former ranges from 0.56 to 181000 mg/L (25th percentile = 834.33 mg/L, median = 1580.16 mg/L, 75th percentile = 3864.08 mg/L, and CV = 222.70%). And the latter from 0.01 to 52915 mg/L (25th percentile = 52.87 mg/L, median = 181.27 mg/L, 75th percentile = 558.73 mg/L, and CV = 264.02%). Furthermore, the results indicate that the detectable medians of the multi-metal concentrations (mg/L) in acid water follow the order: Fe (103.30) > Al (53.90) > Mn (8.1080) > Zn (2.3685) > Cu (0.8010) > Ni (0.2166) > Pb (0.0700) > Cd (0.0220) > Cr (0.0200) > As (0.0108) > Hg (0.0038), while that of the neutral/alkaline water is Mn (0.2164) > Fe (0.1700) > Zn (0.0391) > Al (0.0350) > Cu (0.0100) > Ni (0.0050) > As (0.0034) > Cr (0.0031) > Pb (0.0012) > Cd (0.0004) > Hg (0.0003).

3.1.1 Contents of acid mining-affected water in China

The multi-component concentrations of mining-affected water in both coal and metal mines are displayed in Figs. 3 and S5, and the statistics are given in detail in Table S4. It is obvious that the concentrations of sulfate, Fe, Mn, Al, and several HMs in the mining-affected water of most

metal mines are higher than that of coal mines, especially in mining-affected water with low pH (< 6.5). For acid mining-affected water, the pH of coal mines is approximately 1.90 - 6.50 (with a median of 4.50), while the pH of metal mines is approximately 1.20 - 6.50 (with a median of 3.10). The medians (IQR) of SO_4^{2-} are 1381.59 (871.41, 1954.73) mg/L and 2982.00 (778.15, 10200.00) mg/L for coal mines and metal mines, respectively. In conjunction with Fig. S6, it can be seen that the detectable medians of multi-metal concentrations (mg/L) in coal mining-affected water are 77.41 (Fe), 12.87 (Al), 3.50 (Mn), 0.4211 (Zn), 0.1796 (Ni), 0.0431 (Cu), 0.0080 (Cr), 0.0036 (Cd), 0.0034 (As), 0.0023 (Pb), and 0.0004 (Hg), respectively. Additionally, the detectable medians of multi-metal concentrations (mg/L) in metal mining-affected water are 152.00 (Al), 113.77 (Fe), 15.82 (Mn), 7.200 (Zn), 1.7325 (Cu), 0.2142 (Ni), 0.1498 (Pb), 0.0500 (Cr), 0.0383 (Cd), 0.0281 (As), and 0.0090 (Hg), respectively.

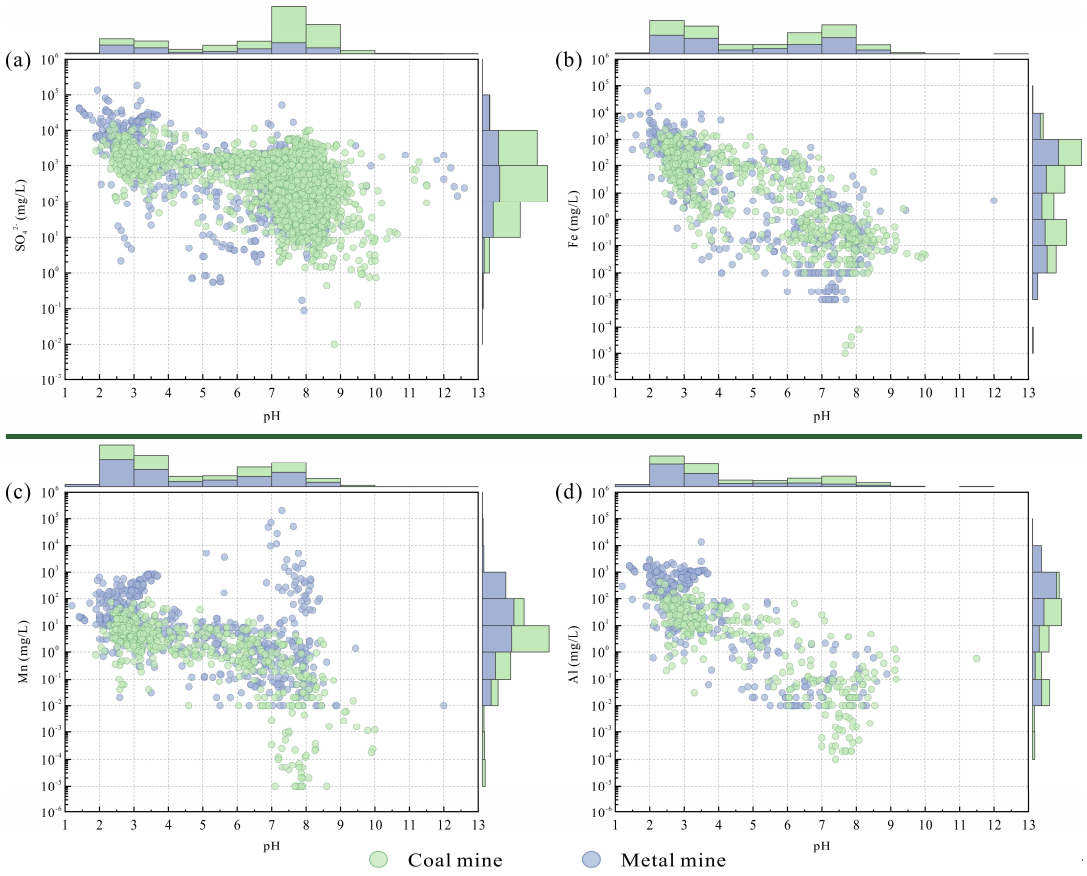

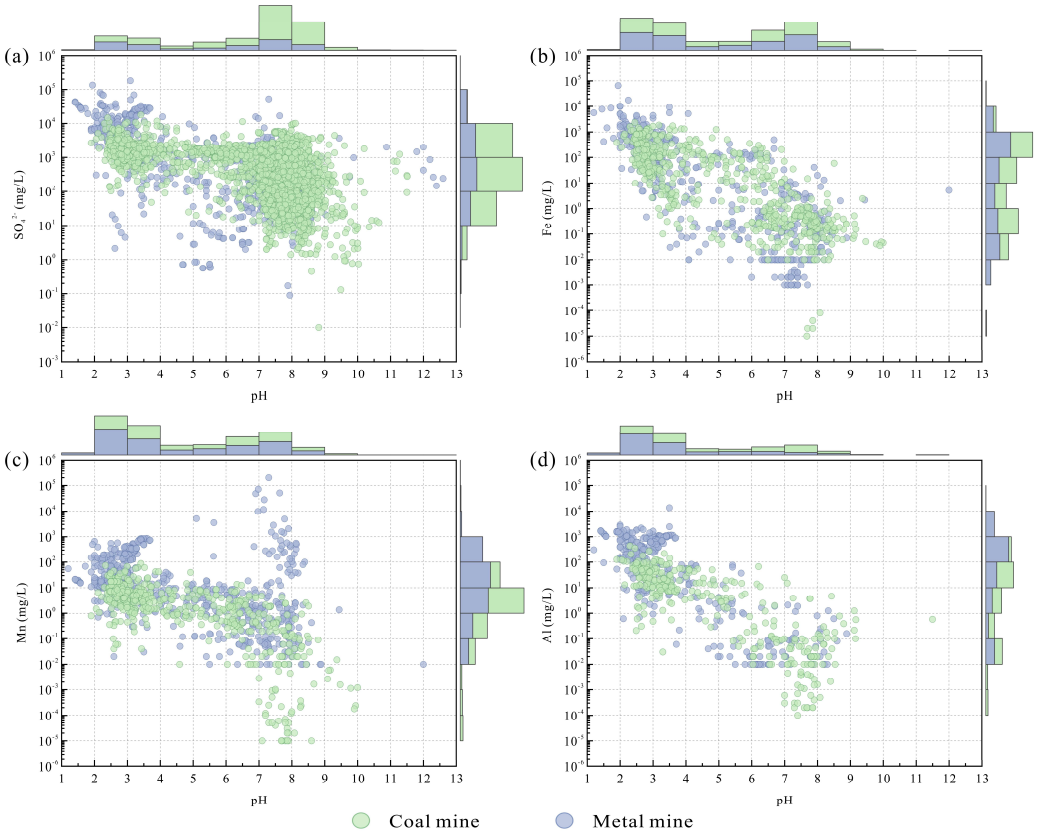

Figure 3. The ~~respective~~ relationship ~~of~~ between pH ~~versus~~ and the respective concentrations including (a) SO_4^{2-}, (b) Fe, (c) Mn, and (d) Al, in coal and metal mines. The binned frequency distribution of the samples is shown along the x and y axes.

3.1.2 Contents of non-acid mining-affected water

Similarly, for non-acid mining-affected water, the pH value of coal mines is about 6.51 - 11.51 (with a median of 7.82), while that of metal mines is about 6.51 - 12.60 (with a median of 7.70). The medians (IQR) of SO_4^{2-} are 193.51 (48.97, 582.70) mg/L and 157.41 (60.23, 425.33) mg/L for coal mines and metal mines, respectively. As shown in Fig. S6, the results indicate that the detectable medians of multi-metal concentrations (mg/L) in coal mines are in the order of Fe (0.2500) > Mn (0.0204) > Al (0.0200) > Zn (0.0048) > Ni (0.0040) > Cr (0.0022) > As (0.0016) > Cu (0.0010) > Pb (0.0003) > Hg (0.0001) > Cd (0.0000), respectively. The detectable median

concentrations (mg/L) of Mn, Zn, Al, Fe, Cu, Pb, Ni, Cr, As, Cd, and Hg in metal mines are 0.7612, 0.0692, 0.0575, 0.0484, 0.0196, 0.0068, 0.0065, 0.0042, 0.0040, 0.0017, and 0.0003, respectively. In addition, the results of non-parametric tests (*i.e.*, Mann-Whitney U-test and Spearman's rank correlation) are presented in the Section S2 (Fig. S7) of the Supplement.

3.2 Spatial patterns of mining-affected water pollution in China

The coal mines surveyed in the study are mainly located in the northern and southwestern regions, which together account for approximately 70% of the national coal production. This localized distribution aligns closely with the pattern of coal-mining belts in China. The southwestern and southern regions of China, rich in metallic mineral resources and with complex geological conditions, have been subject to frequent or unregulated mining activities for many years. Conversely, the western and northern regions are relatively poorly endowed with metal resources (Yu et al., 2024). The mining-affected water is divided into 4 types in the study based on the multi-component characteristic, *i.e.*, with low pH, with high sulfate, with high Fe and Mn, and with high HMs. Given that mining activities have posed great threats to the surface water and groundwater, the classification thresholds incorporated both the distribution of the collected data and regulatory benchmarks from the Environmental Quality Standards for Surface Water (GB 3838-2002) and the Standard for Groundwater Quality (GB/T14848-2017) in China. The categories of water quality in the above documents are listed in Tables S5 and S6. Figs. 4 and S8 showcase the regional patterns of the mining-affected water, and a decreasing trend in pollution levels can be observed from South China to North China.

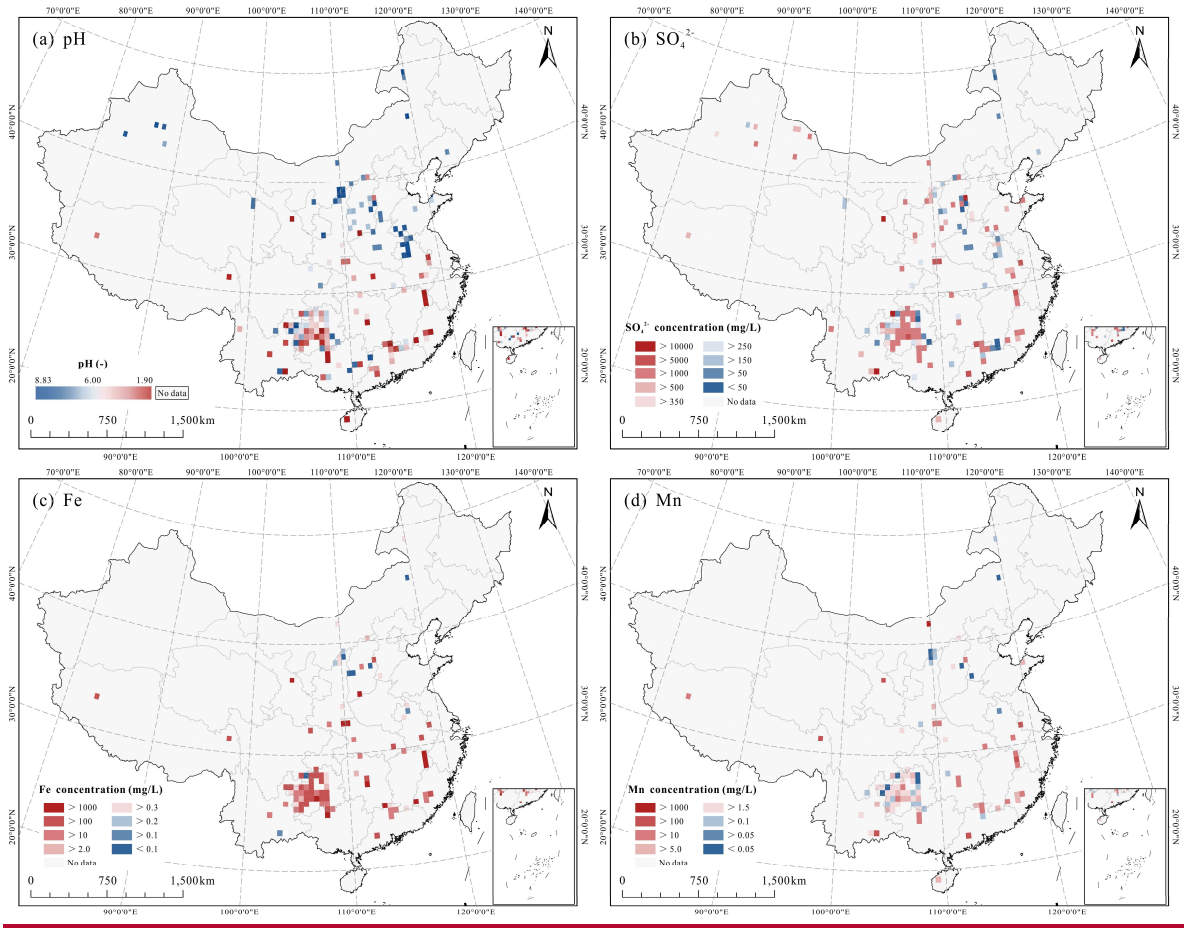
(a) pH
pH (-)
8.83 6.00 1.90
No data
0 750 1,500km
(b) SO_4^{2-}
SO_4^{2-} concentration (mg/L)
> 10000
> 5000
> 1000
> 500
> 350
> 250
> 150
> 50
< 50
No data
(c) Fe
Fe concentration (mg/L)
> 1000
> 100
> 10
> 2.0
No data
> 0.3
> 0.2
> 0.1
< 0.1
(d) Mn
Mn concentration (mg/L)
> 1000
> 100
> 10
> 5.0
No data
> 1.5
> 0.1
> 0.05
< 0.05

287

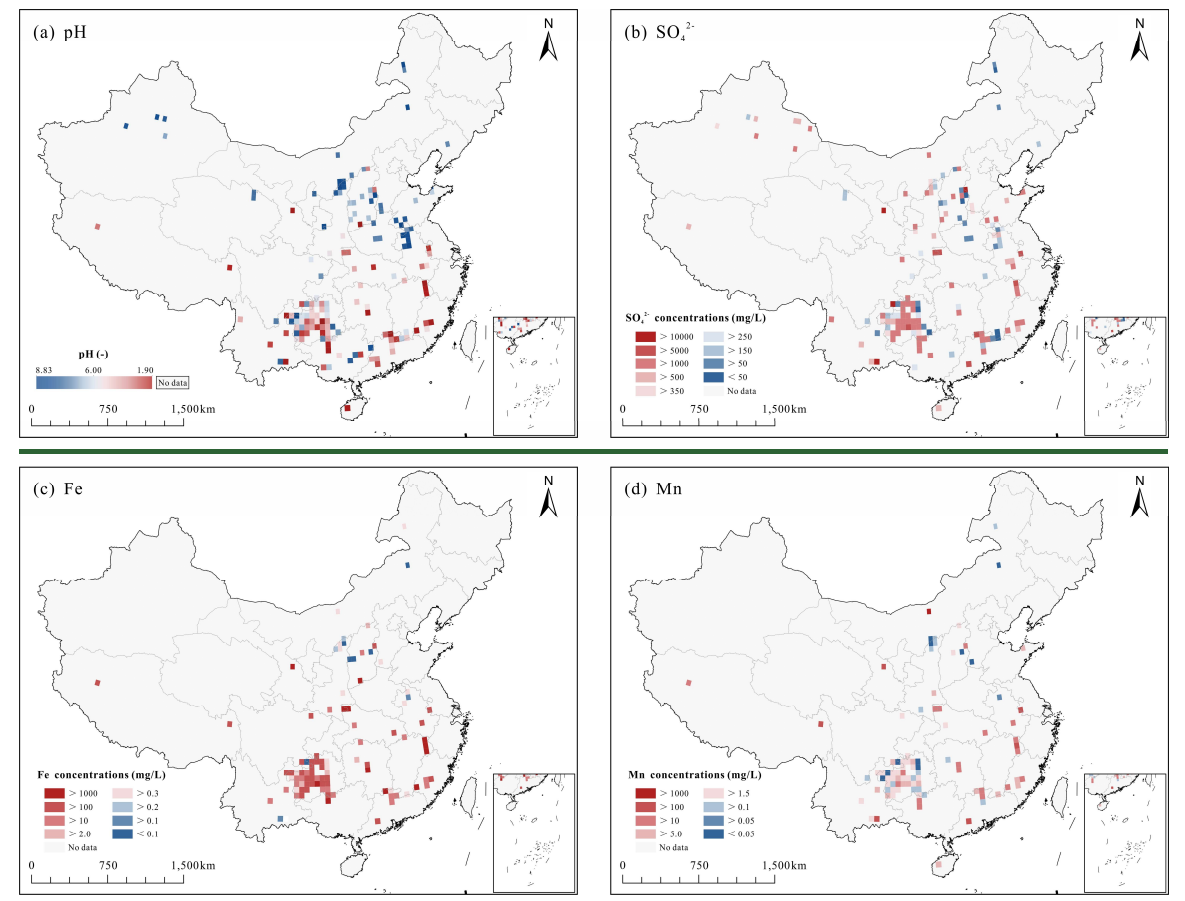
(a) pH
pH (-)
8.83 6.00 1.90
No data
0 750 1,500km
(b) SO_4^{2-}
SO_4^{2-} concentrations (mg/L)
> 10000
> 5000
> 1000
> 500
> 350
> 250
> 150
> 50
< 50
No data
(c) Fe
Fe concentrations (mg/L)
> 1000
> 100
> 10
> 2.0
No data
> 0.3
> 0.2
> 0.1
< 0.1
(d) Mn
Mn concentrations (mg/L)
> 1000
> 100
> 10
> 3.0
No data
> 1.5
> 0.1
> 0.05
< 0.05

288

Figure 4. The spatial distribution of (a) pH; and the mean concentration of individual components (mg/L) showing ~~respective~~ (b) SO_4^{2-}, (c) Fe, and (d) Mn, respectively, in mining-affected water on the 0.5° grid. The classification thresholds for the main components are based on the distribution of all collected data, as well as regulatory benchmarks from GB 3838-2002 and GB/T 14848-2017 in China.

3.2.1 Mining-affected water with low pH

The acid mine water is the predominant contaminant subtype, with pH values significantly below natural freshwater baselines (generally between 2.0 and 4.0). AMD is generally associated with the extraction and processing of sulfur-bearing metalliferous ore deposits (*e.g.*, pyrite, chalcopyrite, pyrrhotite, and sphalerite) and sulfide-rich coal in China (Blowes et al., 2014; Feng et al., 2014). Spatial pattern analysis revealed intense acidification hotspots (pH < 6.5) concentrated in South China, especially in the provinces of Fujian, Guangdong, Guizhou, Hubei, Hunan, Jiangxi, and Yunnan. In particular, the pH of Fuquan City in Guizhou Province reached 1.90, indicating extreme acidity. Combined with the results of the Spearman correlation analysis, a strong geochemical coupling between acidity, sulfate, and dissolved metals can be observed.

3.2.2 Mining-affected water with high sulfate

It is evident that there is a spatial consistency in the distribution of high-sulfate mining-affected water and acid water (Fig. 4b). The quantitative assessment of 138 data grids demonstrates that 73.9% (n = 102) exceed the sulfate threshold concentration of 250 mg/L. In addition, the high sulfate mining-affected water pollution is also particularly prevalent in the provinces/autonomous regions of Anhui, Hebei, Shandong, Shaanxi-Inner Mongolia, and Xinjiang, where the pH values

310 are generally > 6.5. Contrary to typical AMD paradigms, there are two pathways to produce non-
311 acid, high-sulfate water in the neutral/alkaline-pH systems: (i) by pyrite oxidation followed by
312 natural neutralization, and (ii) by dissolution of sulfur-bearing and gypsum minerals. For instance,
313 the Ordovician limestone aquifer is composed of dolomite, which is the primary source of sulfate
314 in southwest Shandong (*e.g.*, Hongshan-Zhaili mines), Anhui (*e.g.*, Huainan-Huaibei mines) and
315 other mining areas. The above-mentioned spatial heterogeneities found in our study are in good
316 agreement with the results of Feng et al. (2014).

317 *3.2.3 Mining-affected water with high Fe and Mn*

318 Nationally, dissolved Fe and Mn concentrations far exceed the Class III threshold for
319 groundwater in China (GB/T14848-2017: Fe > 0.3 mg/L, Mn > 0.1 mg/L). Spatial pattern analysis
320 identifies six critical Fe contamination hotspots (Fig. 4c): Fujian (*e.g.*, Zijinshan copper mine),
321 Guangdong (*e.g.*, Lechang lead-zinc mine), Gansu (*e.g.*, Baiyin copper mine), Hunan (*e.g.*,
322 Shaodong coal mine), Jiangxi (*e.g.*, Dexing/Yongping copper mines) and Shannxi (*e.g.*, Baihe
323 pyrite mine) provinces, where the concentrations even exceed 1000 mg/L. Parallel spatial patterns
324 emerge for Mn contamination (Fig. 4d). Guangdong (*e.g.*, Yunfu pyrite mine), Gansu (*e.g.*, Baiyin
325 copper mine), Inner Mongolia (*e.g.*, Bayan Obo pyrite mine), Jiangxi (*e.g.*, Dexing copper mine),
326 Tibet (*e.g.*, Yulong copper mine) and Yunnan (*e.g.*, Bainiuchang polymetallic mine)
327 provinces/autonomous regions are the severe Mn pollution area. The hydrogeochemical cycling of
328 Fe and Mn in mining-affected aquatic systems is primarily governed by coupled geochemical
329 weathering processes and redox dynamics. Hydrodynamic conditions and water acidity play critical
330 roles in regulating the dissolution efficiency of these metals. It is well recognized that many metal
331 ores naturally contain Fe- and Mn-bearing minerals, which can release metal ions into solution

upon interaction with mine water, particularly under acidic conditions.

3.2.4 Mining-affected water with high heavy metals

For mining-affected waters characterized by elevated concentrations of HMs, including Cr, Ni, Cu, Zn, As, Cd, Hg, and Pb, the identified spatial hotspots are largely consistent, mainly distributed across the Yangtze River Basin as well as the provinces of Fujian, Gansu, Guangdong, and Guangxi (Figs. S8). These regions are well-known as major centers for non-ferrous metal production in China and play a critical role in the national mining industry (Zhang et al., 2016a). Notably, in the present study, the Baiyin copper mine in Gansu Province exhibits extreme levels of Cu, Zn, Cd, Hg, and Pb contamination. The Bainiuchang polymetallic mine, located in the southeastern Yunnan metallogenic belt, is identified as a significant source of Cr and As. In addition, the Zhongtiaoshan copper mining area is found to have the highest recorded concentration of Ni in AMD, reaching 15.0 mg/L.

In connection with the results summarized in Section 3.1, the top four HMs in acid water are Zn, Cu, Ni, and Pb, while that in non-acid water are Zn, Cu, Ni, and As. According to the review by Yin et al. (2018), the mineral composition of copper deposits is complex and includes associated minerals such as nickel, gold, and sulfur. Approximately 76% of the associated gold, 32.5% of the associated silver, and 76% of the sulfur originate from copper mines in China. This reason can explain the prevalence of Cu, Ni, and sulfate contamination hotspots in China's major copper production bases, *i.e.*, Jiangxi (Dexing/Yongping/Dongxiang, etc.), Tongling (Tongguanshan/Shizishan/Xinqiao, etc.), Daye (Tonglushan/Tongshankou, etc.), Zhongtiaoshan, Baiyin, and other copper bases (Chen et al., 2013). Besides, the Zn and Pb pollution levels are relatively higher in the Yunnan-Guizhou and Guangxi-Guangdong regions (Figs. S8d and S8h),

where are abundantly occupied by the lead-zinc ores (*e.g.*, Dachang, Daxin, Wuxu, and Fankou lead-zinc mines, etc.). In these deposits, sphalerite (ZnS) and galena (PbS) are the principal mineral sources of Zn and Pb, respectively (Blowes et al., 2014). With respect to As contamination in mining-affected water, it has been demonstrated that pyrite (FeS_2) may contain substantial amounts of As. Previous studies (Abraitis et al., 2004; Blanchard et al., 2007) have reported that As can substitute for sulfur in the pyrite crystal lattice, forming As-S dianion groups. The incorporation of As into pyrite enhances its chemical reactivity and accelerates its dissolution.

3.3 Risks of mining-affected water in China

Ingestion and dermal contact are the primary exposure pathways for both adults and children residing in mining areas. The risks associated with such exposures are further exacerbated by the persistence, mobility, and bioaccumulative potential of HMs in the environment. Among the metals analyzed in this study, Cr, Ni, As, Cd, and Pb have been classified as carcinogenic to humans by the International Agency for Research on Cancer. In this section, CRs are assessed specifically for Cr, Cd, and As, as carcinogenic slope factors for the other metals are unavailable (Fig. 5).

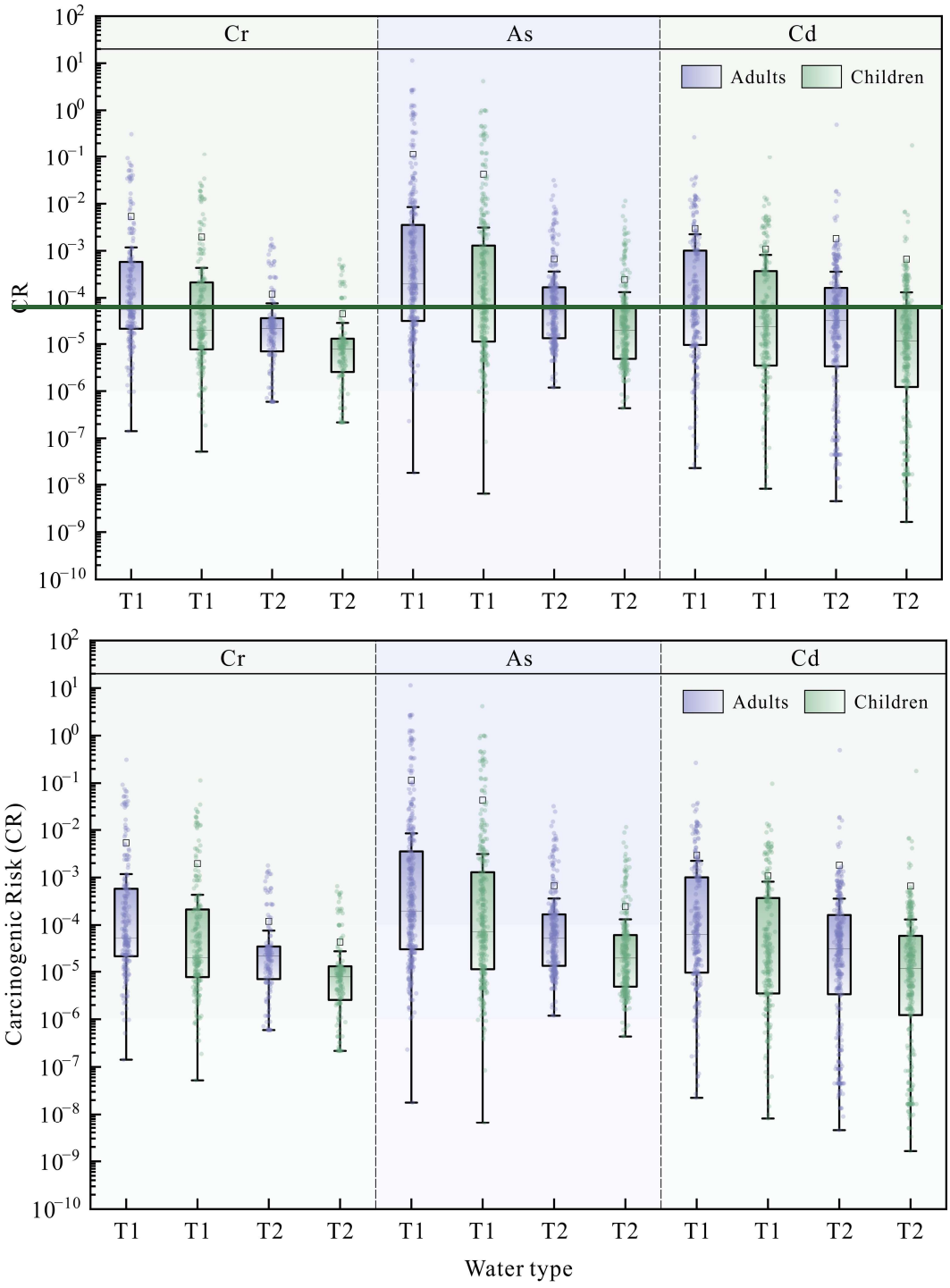

Figure 5. The carcinogenic risk (CR) values of Cr, As, and Cd in mining-affected water. T1 category includes mine drainage, mine water, and leachate water, while T2 category indicates mining-affected surface water and groundwater.

Additionally, Fe, Mn, Cr, Ni, Cu, Zn, As, Cd, and Pb are taken into consideration to calculate

the cumulative NCRs for residents (Fig. 6). To better illustrate the human health risks posed by different types of mining-affected water in China, the risk assessment is categorized into two types: T1 and T2. The T1 category includes mine drainage, mine water, and leachate water, which pose significant threats to the surrounding water systems. The T2 category refers to surface water and groundwater that have been affected by mining activities.

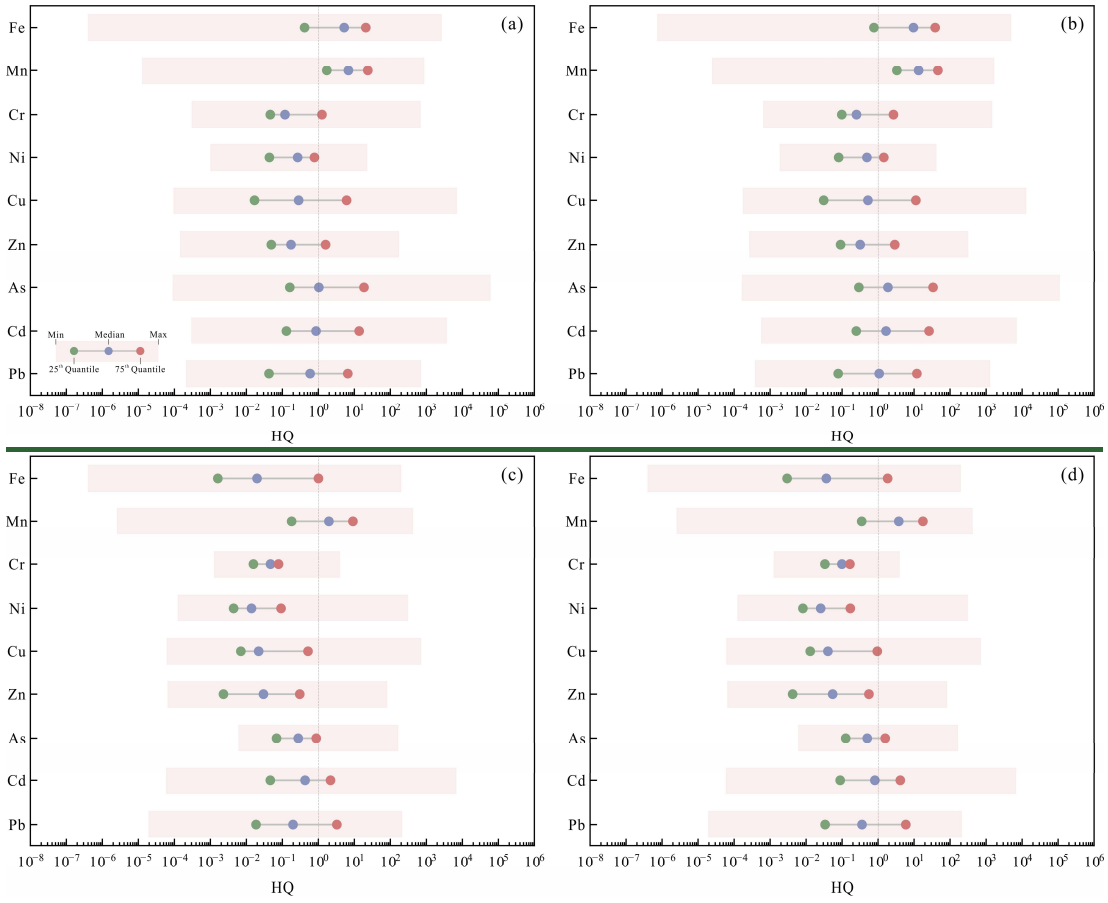

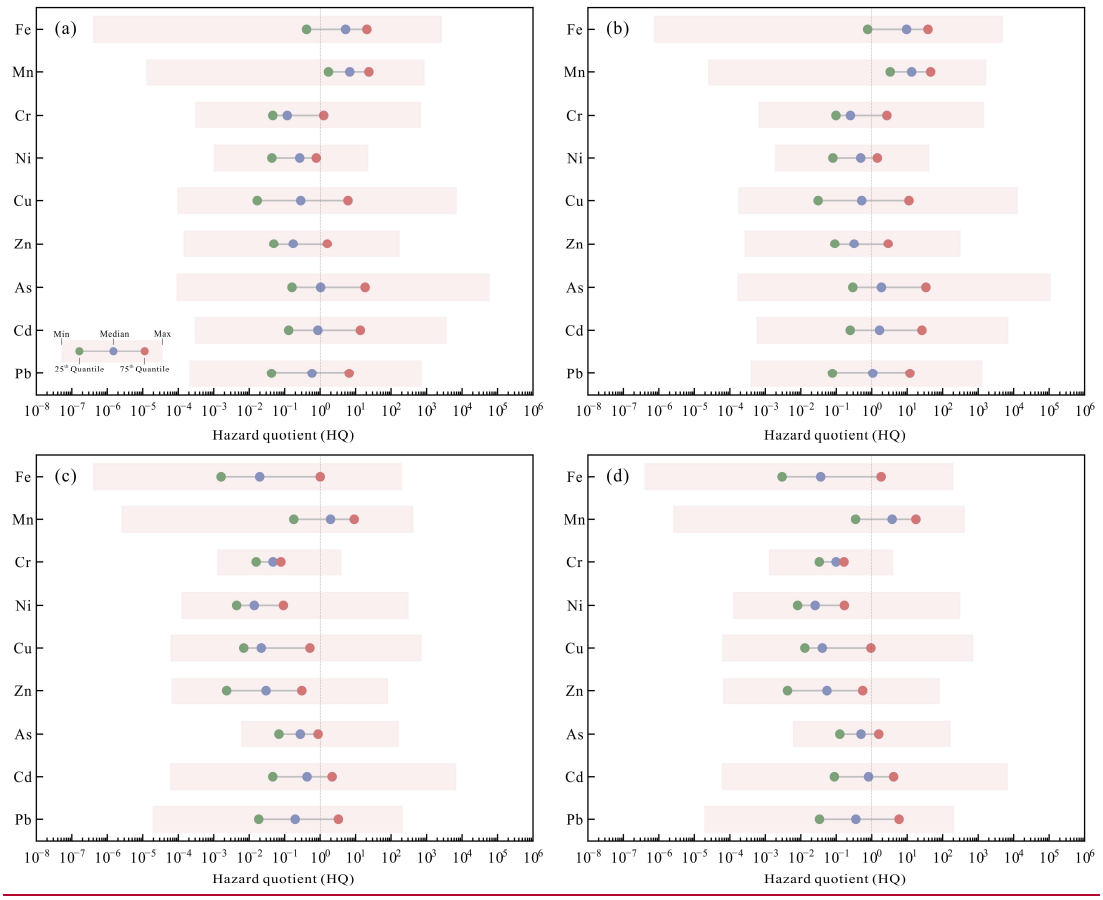

Figure 6. The hazard quotient (HQ) values of Fe, Mn, Cr, Ni, Cu, Zn, As, Cd, and Pb in mining-affected water for (a) T1-Adult, (b) T1-Children, (c) T2-Adult, and (d) T2-Children, respectively. T1 category includes mine drainage, mine water, and leachate water, while T2 category indicates mining-affected surface water and groundwater.

3.3.1 Carcinogenic risk of mining-affected water

According to the guidelines established by the US EPA (2004), CR or TCR values in the range of 10^{-6} to 10^{-4} are considered to be within the acceptable risk range. As shown in Fig. 5, the median CR values for different population groups and water categories generally follow the order As > Cd > Cr. This trend is consistent with the findings of Shi et al. (2018), who reported a similar risk ranking for HMs in soils from mining areas. For T1-type water, the median CR values for all assessed metals are below the upper limit of 10^{-4}, except for As exposure in adults. Specifically, the median

CR values for adults are As (1.98×10^{-4}) > Cd (6.40×10^{-5}) > Cr (5.39×10^{-5}), while for children they are (7.24×10^{-5}) > Cd (2.34×10^{-5}) > Cr (1.97×10^{-5}). In comparison, the CR values associated with T2-type water are generally lower than those for T1-type water. The median values for adults are 5.28×10^{-5} (As), 3.14×10^{-5} (Cd), and 2.13×10^{-5} (Cr), while the corresponding values for children are 1.93×10^{-5} (As), 1.15×10^{-5} (Cd), and 7.82×10^{-6} (Cr). Notably, the median TCR values for both adults and children in the mining areas assessed in this study exceed the upper acceptable limit, reaching 3.02×10^{-4} and 1.10×10^{-4}, respectively. In connection with the results displayed in Fig. S9a, 68.25% of T1-type water samples and 40.27% of T2-type water samples posed non-negligible CRs (TCR > 10^{-4}, driven by the combined effects of Cr, Cd, and As) for adults. The corresponding percentages for children were 51.47% (T1-type) and 23.31% (T2-type), respectively. ~~the mining areas with non-negligible CRs (TCR > 10^{-4}), primarily driven by the combined effects of Cr, Cd, and As, account for 68.25 % of adults and 51.47% of children exposed to T1-type water, and 40.27% of adults and 23.31% of children exposed to T2-type water.~~ In terms of spatial distribution (Fig. S10), the results indicate that TCR values associated with T1-type water exceed the acceptable threshold in 55.00% (for adults) and 40.00% (for children) of the mining areas. For T2-type water, the proportions of mining areas with unacceptable TCR values are 51.52% (for adults) and 29.29% (for children). These results highlight the need for increased attention and targeted management strategies in high-risk areas.

3.3.2 Non-carcinogenic risk of mining-affected water

For T1-type water (Figs. 6a and 6b) with high HQ values (HQ > 1), Mn, Fe, and As are identified as the primary contributors to NCRs. The corresponding median HQ values for adults are 6.84 (Mn), 5.21 (Fe), and 1.03 (As), while the values for children are 13.26 (Mn), 9.63 (Fe),

414 and 1.88 (As), respectively. In addition, for children, the median HQ values of Cd (1.66) and Pb
415 (1.07) also exceed the acceptable limit of 1. In the case of T2-type water (Figs. 6c and 6d), the
416 median HQ values for all assessed metals (except Mn) are below the USEPA threshold for both
417 adults and children. The descending order of median HQ values is as follows: Mn (1.950 for adults,
418 3.752 for children) > Cd (0.424, 0.812) > As (0.274, 0.500) > Pb (0.196, 0.357) > Cr (0.047, 0.099) >
419 Zn (0.030, 0.055) > Cu (0.022, 0.040) > Fe (0.020, 0.036) > Ni (0.014, 0.025). The results suggest
420 that children are more sensitive to the hazardous effects of HM exposure than adults, probably due
421 to the more conservative parameter settings used for children in the risk assessment model. In
422 connection with the results displayed in Fig. S9b, ~~the mining areas with high HI values (HI > 1,~~
423 ~~stemming from synergistic interactions among Fe, Mn, Cr, Ni, Cu, Zn, As, Cd, and Pb) account for~~
424 ~~88.35 % (for adults) and 91.90% (for children) exposed to T1-type water. For T2-type water, the~~
425 ~~corresponding proportions are 55.75% (for adults) and 63.10% (for children).~~ a significant
426 proportion of mining-affected water samples exceed NCR thresholds (HI > 1), with 88.35% of T1-
427 type and 55.75% of T2-type samples posing potential health risks to adults. These risks primarily
428 originated from synergistic interactions among multiple metals (Fe, Mn, Cr, Ni, Cu, Zn, As, Cd,
429 and Pb). Children exhibit even greater vulnerability, with risk exposure percentages increasing to
430 91.90% (T1-type) and 63.10% (T2-type). As depicted in Fig. S11, the southern regions are
431 predominantly identified as NCR hotspots. Specifically, for T1-type water, 89.04% (for adults) and
432 91.78% (for children) of mining areas exceed the acceptable HI threshold, while in the case of T2-
433 type water, the corresponding proportions are 68.07% and 80.67%, respectively.

4 Discussion

4.1 Underlying mechanisms of pronounced mining-affected water pollution in South China

The underlying mechanisms, including climatic conditions, geological factors, and mining practices, determine the spatial patterns of mining-affected water pollution in China, especially in the highly polluted southern regions. In terms of climatic conditions, the average temperature of the coldest month is > 0°C, while that of the hottest month is > 22°C, and the annual average precipitation is generally > 1,000 mm in South China. The high temperature and precipitation create a synergistic accelerator for mine water acidification. Elevated temperatures stimulate acidophilic microbial communities (*e.g.*, *Acidithiobacillus ferrooxidans*), which enhance enzymatic activity that catalyzes sulfide mineral oxidation. Combined with high levels of precipitation, rainfall infiltrates abandoned mines, tailings ponds, and exposed ore bodies, creating a sustained water-oxygen exchange that drives sulfuric acid formation and iron oxidation processes.

In terms of geological factors, the unique geo-environmental settings of South China, characterized by rugged topography, widespread sulfur-rich strata, and high background value of metallic minerals, result in mining-affected water with high acidity and elevated concentrations of sulfate, Fe, Mn, and HMs (Sun et al., 2022). The coal-forming periods of different mines in the South China coalfields are diverse, mainly Triassic, Neoproterozoic, etc., of which the sulfur enrichment exhibits strong links to marine-land interactions. The sustained seawater intrusion-regression cycle results in elevated sulfur contents (predominantly medium and high-sulfur coals) (Ai et al., 2023; Sun et al., 2025). As illustrated in Fig. S2, the coal fields in China exhibit sulfur contents ranging from 0.02% to 10.48%, with South China's coal-bearing areas showing the highest weighted average sulfur content (2.35%), including 29.63% of high-sulfur coal. Comparatively,

those weighted average sulfur contents of coal-bearing areas in Tibet-Western Yunnan, North China, and Northeast China are 0.94%, 0.88%, and 0.86%, respectively (Tang et al., 2015). In addition, as shown in Fig. S3, the metal mineral resources are abundant in the southern region of China, and the water affected by mining practices is often highly toxic, with harmful HMs such as Cd, Pb, Hg, Cr, As, Cu, and so on, endangering the surface water and groundwater systems (Sun et al., 2022).

As to mining practices, especially those involving sulfide-bearing metalliferous ore deposits and sulfide-rich coal mining, are intrinsically associated with AMD. Acid drainage can occur wherever sulfide minerals are excavated and exposed to atmospheric oxygen. The main sulfide minerals in mine wastes are pyrite (FeS_2) and pyrrhotite ($Fe_{1-x}S$), while other associated sulfides are prone to oxidation and release toxic elements, including Al, As, Cd, Co, Cu, Hg, Ni, Pb and Zn, into the water flowing through the mine tailings (Blowes et al., 2014). The oxidation of FeS_2 by atmospheric oxygen can be expressed by Eqs. (8) - (11). Moreover, underground mining is the primary exploitation method in China. Substantial mined-out areas are formed after mining activities, inducing the accumulation of groundwater and the formation of acid mine water. In recent years, the phenomenon has intensified because a number of mines are abandoned without proper closure measures (Jiang et al., 2020).

$$2FeS_2 + 7O_2 + 2H_2O \rightarrow 2Fe^{2+} + 4SO_4^{2-} + 4H^+ \quad (8)$$

$$4Fe^{2+} + O_2 + 4H^+ \rightarrow 4Fe^{3+} + 2H_2O \quad (9)$$

$$Fe^{3+} + 3H_2O \rightarrow Fe(OH)_3 + 3H^+ \quad (10)$$

$$FeS_2 + 14Fe^{3+} + 8H_2O \rightarrow 15Fe^{2+} + 2SO_4^{2-} + 16H^+ \quad (11)$$

4.2 Effects of mining-affected water pollution in China

It is evident that acidic and metal-rich water is widespread in China, especially in the southern

areas (see Fig. 4 above and Fig. S8). As discussed in Section 4.1, the climatic conditions, geological factors, and mining practices all play vital roles in the pronounced mining-affected water pollution in South China. As a consequence, the contaminants pose significant risks to planetary health by degrading surface water and groundwater quality, destroying biodiversity, and threatening human well-being. Fig. 7 summarizes the key processes and adverse impacts of mining-affected water pollution on the water subsystem, soil subsystem, and human health.

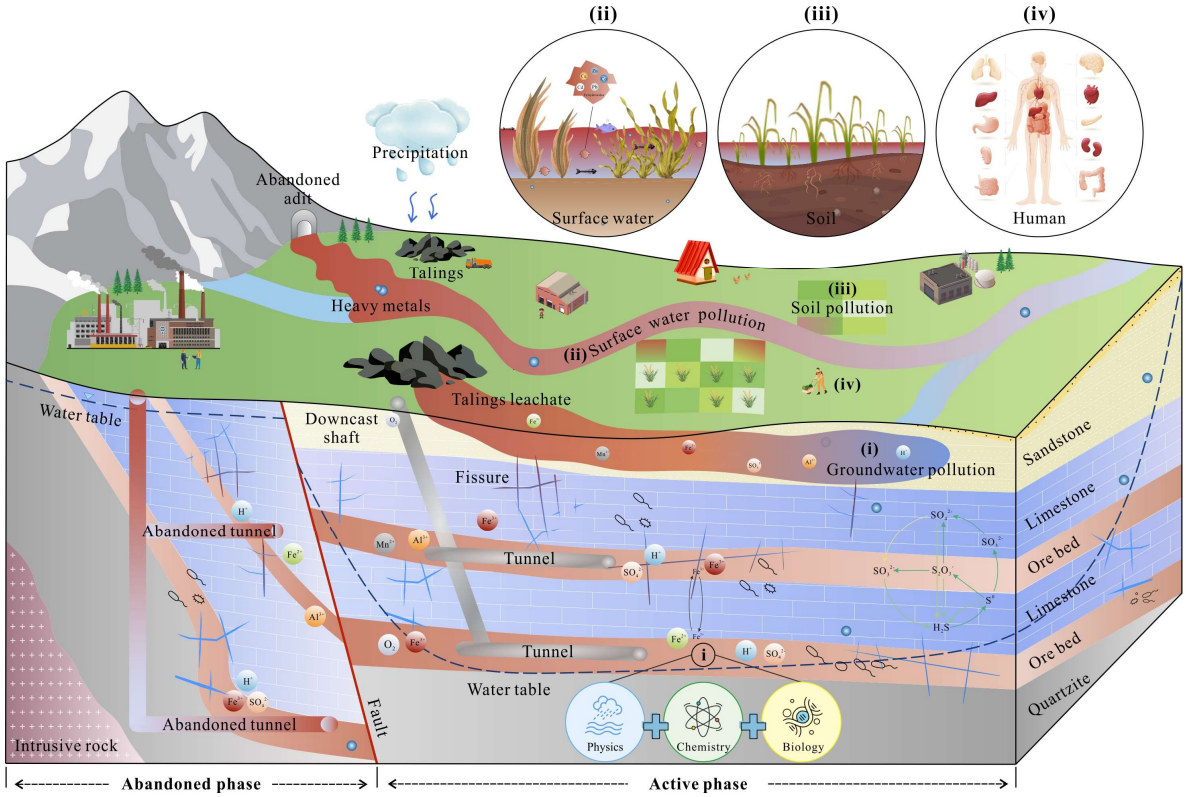

Figure 7. ~~Conceptual model showing the processes and impacts of mining-affected water pollution on (i) groundwater subsystem, (ii) surface water subsystem, (iii) soil subsystem, and (iv) human health.~~Conceptual model illustrating the pollution pathways and environmental impacts of mining-affected water across four key subsystems: (i) groundwater, (ii) surface water, (iii) soil, and (iv) human health, during both active mining and abandoned phases.

***Water subsystem*:** As a vital component of various ecosystems, the water environment faces increasing challenges due to the presence of diverse mining-affected water pollution (as mentioned

in Section 3.2). On the one hand, mining activities can contaminate groundwater, making it unfit for irrigation, drinking, and other purposes. In the active mining phase, the formation of AMD is driven by coupled physical, chemical, and biological processes initiated through sulfide mineral oxidation in the presence of oxygen and water (Fig. 7). These interconnected reactions progressively degrade groundwater quality through acidification and contaminant mobilization (Acharya and Kharel, 2020); In terms of the abandoned phase, the weathering products of exposed sulfides can serve as a source of acidity, sulfate, and dissolved metals, which may subsequently migrate and transform within the recovering groundwater (Blowes et al., 2014). On the other hand, AMD from active and abandoned mines also contaminates water bodies, lowering pH levels and destroying habitats for fish and other aquatic organisms (Ighalo et al., 2021). Toxic metals have the potential to accumulate in the food chain, especially in aquatic organisms, making them one of the most severe contaminants in surface water. Moreover, given that the metals are difficult to biodegrade, their presence has led to detrimental effects on the ecological balance of aquatic ecosystems (Gu et al., 2014; Cui et al., 2021).

***Soil subsystem*:** HMs can enter the soil through mining-affected water runoff and tailings leaching, which have been increasingly detected in soil environments worldwide. Excessive HMs disrupt soil physicochemical properties, impair soil organism viability through physiological dysfunction and behavioral inhibition, and diminish agricultural productivity. Furthermore, these contaminants induce structural shifts in microbial communities, reducing both the abundance and functional diversity of keystone microbial taxa essential for biogeochemical cycling. However, the adverse effects of mining-affected water pollution on the soil subsystem are not the focus of our study. This is because Shi et al. (2023) and Yu et al. (2024) have provided a more comprehensive

514 analysis of the pollution status, risks, and major influencing factors in coal and metal mines across
515 China.

516 ***Human health*:** The results of the human risk assessment presented in Section 3.3 highlight
517 that the CRs and NCRs are severe in China. Moreover, the persistence, high mobility, and
518 bioaccumulation potential of these metals in the environment substantially increase exposure risks,
519 thereby amplifying their adverse health effects. The eight HMs examined in this study exhibit
520 intrinsic toxicity, posing risks to human health through bioaccumulation pathways. Mechanistically,
521 these HMs bind to DNA strands and enzyme-active sites, inducing disruptions in cellular
522 homeostasis, endocrine signaling, immune responses, neurophysiological functions, and
523 reproductive-endocrine systems (Shi et al., 2023; Meng et al., 2024). For example, various injuries
524 linked to Cr exposure include nasal irritation and ulceration, skin irritation, and perforation of the
525 eardrum. Acute exposure to Ni can result in damage to the kidneys, liver, and brain, whereas
526 chronic exposure can cause tissue damage. Respiratory problems, dizziness, nausea, and diarrhea
527 are common symptoms induced by elevated Cu concentrations (Gujre et al., 2021). Zn has a
528 significant capacity for bioaccumulation, leading to increased health risks to the immune and
529 nervous systems via the water-food chain (Cui et al., 2021). Chronic exposure to As is associated
530 not only with skin lesions and skin cancer, but also with neurological, respiratory, cardiovascular,
531 and developmental effects (Zhang et al., 2024). Poisoning with Cd can cause damage to the kidneys,
532 bones, lungs, and liver, and can even lead to cancer. (Feng et al., 2022; Liu et al., 2024). Hg can
533 lead to serious neurological disorders in both children and adults (Rui et al., 2017). Cardiovascular,
534 central nervous system, kidney, and fertility problems are usually associated with Pb exposure (Shi
535 et al., 2023). Furthermore, it has recently been demonstrated that Fe is linked to pathological

disorders such as Alzheimer's and Parkinson's diseases (Sahoo and Sharma, 2023).

4.3 Implications for China's future differentiated management

In the mining areas, the rising HMs contamination and potential health risks in surface water and groundwater call for targeted and forward-looking control strategies in China. In fact, mining regulations differ across provinces and countries, highlighting the need for site-specific frameworks and criteria. Although management may vary by location, priorities must include land use history, mine type, available technology, eco-hydrological conditions, socio-economic factors, multi-stakeholder cooperation, long-term monitoring, effective enforcement of effluent limits, and treatment standards (Acharya and Kharel, 2020). Therefore, the differentiated management in the current study is an optimized regulatory paradigm that customizes strategies to mine types (coal vs. metal) and operational status (active vs. abandoned) based on hydrogeological conditions, pollution source characteristics, and multi-system sustainability requirements. The initiative aims to implement targeted intervention and precise prevention/control to mitigate pollution risks, restore and enhance ecological functions, while concurrently safeguarding human health.

***Coal mine and metal mine*:** The results imply that the water pollution status in metal mines is higher than in coal mines (Figs. 3 and S5). To some extent, policymakers should enhance their focus on regulating metal mining water contamination and devise more effective measures to reduce exposure and manage risks. The results presented in Section 3.1 imply that the characteristic contaminants in the acid water of coal mines are sulfate (with a median of 1381.59 mg/L), Fe (77.41 mg/L), and Mn (3.50 mg/L), while that of metal mines also include a variety of HMs, such as Zn (7.20 mg/L), Cu (1.73 mg/L), Ni (0.21 mg/L), Pb (0.15 mg/L) and so on. Consequently, water quality monitoring frameworks and remediation technologies should adopt site-specific strategies

to account for divergent pollutant profiles in metalliferous and coal mines. These customized approaches should integrate contaminant sources, migration pathways, and ecotoxicological impacts to ensure remediation effectiveness. Some studies have demonstrated that precipitation and neutralization are commonly used methods in coal mines, while more complex technologies, such as ion exchange or membrane separation techniques, are required to remove HMs in metal mines.

***Active mine and abandoned mine*:** The differentiated management policies for active and abandoned mines aim to protect both the environment and public health across different stages of mining operations. Active mining operations require AMD prevention frameworks focusing on source control through sulfide oxidation suppression during the ore extraction and transport cycles. This requires high-frequency sensor networks for real-time contaminant flux tracking and adaptive mitigation protocols. In contrast, abandoned mine management prioritizes remediation-performance validation, integrating long-term hydrogeochemical stability monitoring with ecosystem resilience metrics. In addition, more scientific restoration strategies are critical to rebuilding the sustainable development of the water subsystem and the soil subsystem disrupted by legacy metal loads. Sustainable management also plays a pivotal role in addressing the challenges of mining-related water pollution. Emphasis should be directed to multidisciplinary partnerships and cost-effective and eco-friendly treatments, especially integrated treatment approaches that take into account the synergy of source control and end-of-pipe treatment. These elements are crucial for better understanding the complexities of mine drainage, controlling water quality degradation, and minimizing socio-economic damage.

4.4 Reliability, limitations and prospects

To reveal the nationwide pollution status, spatial heterogeneity, health risks, and effects of

mining-affected water in China, a total of 8,433 water samples from 298 mines were integrated. Additionally, the combination of data mining and quality assessment was employed to enhance the reliability of the available data and build a high-quality database. However, there are still some non-negligible limitations or uncertainties in the study.

On the one hand, the boundaries of mine sites are rarely clearly defined in the literature we collected, which means that the spatial heterogeneity of mining-affected water pollution cannot be accurately represented. On the other hand, the gridded data imply the southern regions, particularly the provinces/autonomous regions of Guizhou, Guangdong, Fujian, Jiangxi, Hunan, and Guangxi, are mining-affected water pollution hotspots. When compared with the reported sample sizes (Fig. S4), this suggests that these areas are generally high-sampling zones, which may potentially distort the representation of distribution. Therefore, it is of great importance to address the bias by (i) combining the data mining and field sampling methods to investigate the potential contamination levels in more coal and metal mines across China; (ii) balancing the sampling density within each zone using bias correction techniques (*e.g.*, kernel density estimation and stratified spatial resampling) to ensure the data representation; and (iii) incorporating spatial uncertainty into the criteria to improve the spatial robustness for the assessments of mining-affected water pollution.

It is noteworthy that we cannot uncover the temporal evolution of mining-affected water pollution due to the varying time scales of the data. Temporal variations in water chemistry (*e.g.*, seasonal fluctuations and monsoon events) significantly impact the environmental fate of contaminants and health risks through multiple mechanisms. During the monsoon season, heavy rainfall flushes tailings ponds or open-pit mines, causing instantaneous spikes in HMs (*e.g.*, Cd, Cr, and As) and sulfate concentrations. Meanwhile, the elevated groundwater levels associated with

high precipitation infiltration drive contaminant plumes along preferential pathways. These dynamics introduce systematic biases into traditional static risk assessments. The annual or quarterly average risk assessment model may underestimate short-term high-dose exposure risks. Moreover, some gridded data only reflect the historical pollution status of a specific mine (*e.g.*, the Suichang gold mine and the coal mines in the Yudong River Basin) that has undergone successful ecological remediation and achieved good water quality levels after mining activities ceased.

Future in-depth research could focus on (i) gathering globally reported data through deep mining and quality control and establishing a high-quality global database to better understand the characteristics of mining-affected water pollution worldwide; (ii) identifying the key factors that govern the transport and transformation of contaminants in surface water and groundwater systems, during active and abandoned periods, and in coal and metal mines; (iii) enhancing the sustainable development of coal and metal mines by AI-driven digital simulations and digital twins, which can provide data-driven insights, optimize remediation endeavors, and advocate proactive measures to safeguard the environment; and (iv) strengthening the studies on the synergistic measures (not only at small-scale experimental sites but also at the mine site scale) to alleviate multifaceted environmental challenges in the mining-affected water and achieve the development of green mining.

5 Conclusions

In this study, the national status, spatial patterns, potential human health risks, and their multifaceted implications of mining-affected water pollution have been elucidated. The new and unique contributions of the current study are: (i) establishing a national-scale high-quality database covering 8,433 surface water or groundwater samples (6,175 coal mine water samples and 2,258

metal mine water samples) from 298 mines (211 coal mines and 87 metal mines) in 26 provinces/autonomous regions of China; and (ii) filling the gap of the nationwide spatial patterns of water pollution and associated health risks from both coal and metal mining activities for the first attempt. Specifically, eight heavy metals (*i.e.*, Cr, Ni, Cu, Zn, As, Cd, Hg, and Pb) are considered in the current study. The main results are as follows:

- The predominant contaminants in both coal and metal mines in China are Zn, Ni and Cu. The detectable concentrations of several heavy metal~~HM~~s are higher in most metal mines than in coal mines, especially in mining-affected water with low pH (< 6.5).
- The order of detectable median values of water affected by coal mining is Zn (0.4211) > Ni (0.1796) > Cu (0.0431) > Cr (0.0080) > Cd (0.0036) > As (0.0034) > Pb (0.0023) > Hg (0.0004), while that of water affected by metal mining is Zn (7.200) > Cu (1.7325) > Ni (0.2142) > Pb (0.1498) > Cr (0.0500) > Cd (0.0383) > As (0.0281) > Hg (0.0090).
- The pollution hotspots and potential risks of mining-affected water (with low pH, high sulfate, Fe, Mn, and heavy metal~~HM~~s) are pronounced in the southern regions due to the synergistic mechanisms of climatic conditions, geological factors, and mining practices, especially in Guizhou, Guangdong, Fujian, Jiangxi, Hunan, and Guangxi provinces/autonomous regions.
- The unacceptable carcinogenic risks caused by poor-quality surface water and groundwater are observed in 51.52% (for adults) and 29.29% (for children) of the mining areas. Moreover, severe non-carcinogenic risks are also identified in 68.07% and 80.67% of mining areas for adults and children, respectively.

Accordingly, the findings of the study yield critical insights for designing differentiated management measures and formulating spatially-adaptive pollution control strategies across three

key dimensions, including geographic scales (site-specific scale, provincial scale, or national scale), mine types (coal or metal), and mining status (active or abandoned). This multidimensional framework enables policymakers to strategically balance the trade-off between green mining activities and human health priorities.

Data availability. The detailed data information can be found in Table S1.

Author contributions. ZYY, JS, JFW, and YY conceptualized the manuscript and its scope. ZYY, DGL, and YYS collected the data. ZYY prepared the initial manuscript with contributions from all co-authors. JS, JFW, YY, YYS, and JCW revised the manuscript.

Competing interests. The authors declare that they have no conflict of interest.

Acknowledgements. The authors are profoundly grateful to Editor Gabriel Rau and the three anonymous reviewers for their insightful and constructive comments, which have greatly enhanced the quality and clarity of the manuscript.

Financial support. This research is financially supported by the National Key Research and Development Program of China (2022YFC3702200), the China National Postdoctoral Program for Innovative Talents (BX20240165), the Jiangsu Funding Program for Excellent Postdoctoral Talents (2024ZB125), and the Fundamental Research Funds for the Central Universities (14380228).

References

Abraitis, P. K., Pattrick, R. A. D., and Vaughan, D. J.: Variations in the compositional, textural and electrical properties of natural pyrite: A review, Int. J. Miner. Process., 74, 41-59, https://doi.org/10.1016/j.minpro.2003.09.002, 2004.

Acharya, B. S. and Kharel, G.: Acid mine drainage from coal mining in the United States – An overview – , J. Hydrol., 588, 125061, https://doi.org/10.1016/j.jhydrol.2020.125061, 2020.

Ai, Y. L., Chen, H. P., Chen, M. F., Huang, Y., Han, Z. T., Liu, G., Gao, X. B., Yang, L. H., Zhang, W. Y., Jia, Y. F., and Li, J.: Characteristics and treatment technologies for acid mine drainage from abandoned coal mines in major coal-producing countries – , J. China Coal Soc., 48(12), 4521-4535 (in Chinese with English abstract), https://doi.org/10.13225/j.cnki.jccs.2022.1846, 2023.

Blanchard, M., Alfredsson, M., Brodholt, J., Wright, K., Richard, C., and Catlow, A.: Arsenic incorporation into FeS_2 pyrite and its influence on dissolution: A DFT study – , Geochim Cosmochim Acta, 71, 624-630, https://doi.org/10.1016/j.gca.2006.09.021, 2007.

Blowes, D. W., Ptacek, C. J., Jambor, J. L., Weisener, C. G., Paktunc, D., Gould W. D., and Johnson, D. B.: The geochemistry of acid mine drainage – , Treatise on Geochemistry (Second Edition), 11, 131-190, https://doi.org/10.1016/B978-0-08-095975-7.00905-0, 2014.

Chen, D., Chen, Y. -P., and Lin, Y.: Heavy rainfall events following the dry season elevate metal contamination in mining-impacted rivers: A case study of Wenyu River, Qinling, China – , Arch. Environ. Contam. Toxicol., 81, 335-345, https://doi.org/10.1007/s00244-021-00870-y, 2021.

Chen, J. P., Zhang, Y., Wang, J. X., Xiao, K. Y., Lou, D. B., Ding, J. H., Yin, J. N., and Xiang, J.: On present situation and potential analysis of copper resources in China – , J. Geol., 37, 358-365 (in Chinese with English abstract), https://doi.org/10.3969/j.issn.1674-3636.2013.03.358, 2013.

Cheng, S.: Heavy metal pollution in China: origin, pattern and control – , Environ. Sci. Pollut. Res., 10(3), 192-198 – , https://doi.org/10.1065/espr2002.11.141.1, 2003.

690 Cui, L., Wang, X. N., Li, J., Gao, X. Y., Zhang, J. W., and Liu, Z. T.: Ecological and health risk
691 assessments and water quality criteria of heavy metals in the Haihe River. , Environ. Pollut.,
692 290, 117971, https://doi.org/10.1016/j.envpol.2021.117971, 2021.
693 Dippong, T., Resz, M. -A., Tănăselia, C., and Cadar, O.: Assessing microbiological and heavy metal
694 pollution in surface waters associated with potential human health risk assessment at fish
695 ingestion exposure. , J. Hazard. Mater., 476, 135187,
696 https://doi.org/10.1016/j.jhazmat.2024.135187, 2024.
697 Dong, F., Yin, H., Cheng, W., Li, Y., Qiu, M., Zhang, C., Tang, R., Xu, G., and Zhang, L.: Study on
698 water inrush pattern of Ordovician limestone in North China Coalfield based on
699 hydrochemical characteristics and evolution processes: A case study in Binhu and Wangchao
700 Coal Mine of Shandong Province, China. , J. Clean. Product., 380, 134954,
701 https://doi.org/10.1016/j.jclepro.2022.134954, 2022.
702 Feng, Q., Li, T., Qian, B., Zhou, L., Gao, B., and Yuan, T.: Chemical Characteristics characteristics
703 and Utilization utilization of Coal coal Mine mine Drainage drainage in China. , Mine Water
704 Environ., 33, 276-286, https://doi.org/10.1007/s10230-014-0271-y, 2014.
705 Feng, S., Deng, S., Tang, Y., Liu, Y., Yang, Y., Xu, S., Tang, P., Lu, Y., Duan, Y., Wei, J., Liang, G.,
706 Pu, Y., Chen, X., Shen, M., and Yang, F.: Microcystin-LR combined with cadmium exposures
707 and the risk of chronic kidney disease: a case-control study in central China. , Environ. Sci.
708 Technol., 56 (22), 15818-15827, https://doi.org/10.1021/acs.est.2c02287, 2022.
709 Gu, D. Z., Li, J. F., Cao, Z. G., Wu, B. Y., Jiang, B. B., Yang, Y., Yang, J., and Chen, Y. P.:
710 Technology and engineering development strategy of water protection and utilization of coal

711 mine in China—, J. China Coal Soc., 46(10), 3079-3089 (in Chinese with English abstract),
712 https://doi.org/10.13225/j.cnki.jccs.2021.0917, 2021.
713 Gu, Y. G., Li, Q. S., Fang, J. H., He, B. Y., Fu, H. B., and Tong, Z. J.: Identification of heavy metals
714 sources in the reclaimed farmland soils of the pearl estuary in China using a multivariate
715 geostatistical approach———, ____Ecotox. Environ. Saf., 105, 7-12,
716 https://doi.org/10.1016/j.ecoenv.2014.04.003, 2014.
717 Gujre, N., Rangan, L., and Mitra, S.: Occurrence, geochemical fraction, ecological and health risk
718 assessment of cadmium, copper and nickel in soils contaminated with municipal solid wastes—,
719 Chemosphere, 271, 129573, https://doi.org/10.1016/j.chemosphere.2021.129573, 2021.
720 Gunson, A. J. and Jian, Y.: Artisanal mining in the People's Republic of China—, International
721 Institute of Environment and Development, 2001.
722 Havig, J. R., Grettenberger, C., and Hamilton, T. L.: Geochemistry and microbial community
723 composition across a range of acid mine drainage impact and implications for the Neoarchean-
724 Paleoproterozoic transition———, ___J. Geophys. Res. Biogeosci., 122, 19,
725 https://doi.org/10.1002/2016JG003594, 2017.
726 He, B., Yun, Z. J., Shi, J. B., and Jiang, G. B.: Research progress of heavy metal pollution in China:
727 Sources, analytical methods, status, and toxicity—, Chin. Sci. Bull., 58(2), 134-140,
728 https://doi.org/10.1007/s11434-012-5541-0, 2013.
729 He, M., Wang, Z., and Tang, H.: The chemical, toxicological and ecological studies in assessing
730 the heavy metal pollution in Le An River, China—, Water Res., 32(2), 510-518,
731 https://doi.org/10.1016/S0043-1354(97)00229-7, 1998.

Hou, Y., Zhao, Y., Lu, J., Wei, Q., Zang, L., and Zhao, X.: Environmental contamination and health risk assessment of potentially toxic trace metal elements in soils near gold mines – A global meta-analysis, Environ. Pollut., 330, 121803, https://doi.org/10.1016/j.envpol.2023.121803, 2023.

Hou, Z., Huang, L., Zhang, S., Han, X., Xu, J., and Li, Y.: Identification of groundwater hydrogeochemistry and the hydraulic connections of aquifers in a complex coal mine, J. Hydrol., 628, 130496, https://doi.org/10.1016/j.jhydrol.2023.130496, 2024.

Hu, H., Jin, Q., and Kavan, P.: A study of heavy metal pollution in China: Current status, pollution-control policies and countermeasures, Sustainability, 6, 5820-5838, https://doi.org/10.3390/su6095820, 2014.

Hu, R. Z., Liu, J. M., and Zhai, M. G.: Mineral resources science in China: a roadmap to 2050, Science Press, Beijing, 2009.

Ighalo, J. O. and Adeniyi, A. G.: A comprehensive review of water quality monitoring and assessment in Nigeria, Chemosphere 260, 127569, https://doi.org/10.1016/j.chemosphere.2020.127569, 2020.

Ighalo, J. O., Kurniawan, S. B., Iwuozor, K. O., Aniagor, C. O., Ajala, O. J., Oba, S. N., Iwuchukwu, F. U., Ahmadi, S., and Igwegbe, C. A.: A review of treatment technologies for the mitigation of the toxic environmental effects of acid mine drainage (AMD), Process Safe. Environ. Protect., 157, 37-58, https://doi.org/10.1016/j.psep.2021.11.008, 2022.

Jiang, C. F., Gao, X. B., Hou, B. J., Zhang, S. T., Zhang, J. Y., Li, C. C., and Wang, W. Z.: Occurrence and environmental impact of coal mine goaf water in karst areas in China, J. Cleaner Product., 275, 123813, https://doi.org/10.1016/j.jclepro.2020.123813, 2020.

754 Kumar, V., Paul, D., and Kumar, S.: Acid mine drainage from coal mines in the eastern Himalayan
755 sub-region: Hydrogeochemical processes, seasonal variations and insights from hydrogen and
756 oxygen stable isotopes——, Environ. Res., 252, Part 4, 119086,
757 https://doi.org/10.1016/j.envres.2024.119086, 2024.
758 Li, Z., Ma, Z., van der Kuijp, T. J., Yuan, Z., and Huang, L.: A review of soil heavy metal pollution
759 from mines in China: Pollution and health risk assessment—, Sci. Total Environ., 468-469,
760 843-853, https://doi.org/10.1016/j.scitotenv.2013.08.090, 2014.
761 Liu, T., Yuan, X., Luo, K., Xie, C, and Zhou, L.: Molecular engineering of a new method for
762 effective removal of cadmium from water——, Water Res., 253, 121326,
763 https://doi.org/10.1016/j.watres.2024.121326, 2024.
764 Liu, X., Shi, H., Bai, Z., Zhou, W., Liu, K., Wang, M., and He, Y.: Heavy metal concentrations of
765 soils near the large opencast coal mine pits in China—, Chemosphere, 244, 125360,
766 https://doi.org/10.1016/j.chemosphere.2019.125360, 2020.
767 Ma, R., Gao, J., Guan, C., and Zhang, B.: Coal mine closure substantially increases terrestrial water
768 storage in China—, Commun. Earth Environ., 5, 418, https://doi.org/10.1038/s43247-024-
769 01589-z, 2024.
770 Meng, F., Cao, R., Zhu, X., Zhang, Y., Liu, M., Wang, J., Chen, J., and Geng, N.: A nationwide
771 investigation on the characteristics and health risk of trace elements in surface water across
772 China—, Water Res., 250, 121076, https://doi.org/10.1016/j.watres.2023.121076, 2024.
773 Moodley, I., Sheridan, C. M., Kappelmeyer, U., and Akcil, A.: Environmentally sustainable acid
774 mine drainage remediation: Research developments with a focus on waste/by-products—,
775 Miner. Eng., 126, 207-220, https://doi.org/10.1016/j.mineng.2017.08.008, 2018.

776 Qu, S., Liang, X., Liao, F., Mao, H., Xiao, B., Duan, L., Shi, Z., Wang, G., and Yu, R.: Geochemical
777 fingerprint and spatial pattern of mine water quality in the Shaanxi-Inner Mongolia Coal Mine
778 Base, Northwest China——, Sci. Total Environ., 854, 158812,
779 https://doi.org/10.1016/j.scitotenv.2022.158812, 2023.
780 Rui, L., Han, W., Jing, D., Fu, W., and Yi, L.: Mercury pollution in vegetables, grains and soils
781 from areas surrounding coal-fired power plants——, Sci. Rep., 7, 1-9,
782 https://doi.org/10.1038/srep46545, 2017.
783 Sahoo, K. and Sharma, A.: Understanding the mechanistic roles of environmental heavy metal
784 stressors in regulating ferroptosis: adding new paradigms to the links with diseases——,
785 Apoptosis, 28(3), 277-292, https://doi.org/10.1007/s10495-022-01806-0, 2023.
786 Shi, J., Zhao, D., Ren, F., and Huang, L.: Spatiotemporal variation of soil heavy metals in China:
787 The pollution status and risk assessment——, Sci. Total Environ., 871, 161768,
788 https://doi.org/10.1016/j.scitotenv.2023.161768, 2023.
789 Sun, J., Tang, C., Wu, P., Liu, C., and Zhang, R.: Migration of Cu, Zn, Cd and As in epikarst water
790 affected by acid mine drainage at a coalfield basin, Xingren, Southwest China——, Environ. Earth
791 Sci., 69, 2623-2632, https://doi.org/10.1007/s12665-012-2083-3, 2013.
792 Sun, Y. J., Chen, G., Xu, Z. M., Yuan, H. Q., Zhang, Y. Z., Zhou, L. J., Wang, X., Zhang, C. H., and
793 Zheng, J. M.: Research progress of water environment, treatment and utilization in coal
794 mining areas of China——, J. China Coal Soc., 45(1), 304-316 (in Chinese with English abstract),
795 https://doi.org/10.13225/j.cnki.jccs.YG19.1654, 2020.
796 ~~Sun, Y.J., Guo, J., Xu, Z.M., Zhang, L., Chen, G., Xiong, X.F., Hua, J.F., Mu, L.J., and Wu, W.X.:~~
797 ~~Spatial distribution characteristics of mine water quality in coal mining areas of China and~~

~~technological approaches for mine water treatment. J. China Coal Soc., 50(1), 584-599 (in Chinese with English abstract), https://doi.org/10.13225/j.cnki.jccs.YG24.1547, 2025.~~

Sun, Y. J., Zhang, L., Xu, Z. M., Chen, G., Zhao, X. M., Li, X., Gao, Y. T., Zhang, S. G., and Zhu, L. L.: Multi-field action mechanism and research progress of coal mine water quality formation and evolution~~.~~, J. China Coal Soc., 47(1), 423-437 (in Chinese with English abstract), https://doi.org/10.13225/j.cnki.jccs.YG21.1937, 2022.

Sun, Y. J., Guo, J., Xu, Z. M., Zhang, L., Chen, G., Xiong, X. F., Hua, J. F., Mu, L. J., and Wu, W. X.: Spatial distribution characteristics of mine water quality in coal mining areas of China and technological approaches for mine water treatment, J. China Coal Soc., 50(1), 584-599 (in Chinese with English abstract), https://doi.org/10.13225/j.cnki.jccs.YG24.1547, 2025.

USEPA: Risk assessment guidance for superfund, Volume I: Human health evaluation manual final~~.~~, U.S. Environment Protection Agency (Washington DC), 2004.

USEPA: Exposure factors handbook~~.~~, U.S. Environment Protection Agency (Washington DC), 2011.

Wang, M., Wang, X., Zhou, S., Chen, Z., Chen, M., Feng, S., Li, J., Shu, W., and Cao, B.: Strong succession in prokaryotic association networks and community assembly mechanisms in an acid mine drainage-impacted riverine ecosystem~~.~~, Water Res., 243, 120343, https://doi.org/10.1016/j.watres.2023.120343, 2023.

Wang, Y., Dong, R., Zhou, Y., and Luo, X.: Characteristics of groundwater discharge to river and related heavy metal transportation in a mountain mining area of Dabaoshan, Southern China~~.~~, Sci. Total Environ., 679, 346-358, https://doi.org/10.1016/j.scitotenv.2019.04.273, 2019.

819 Wei, J., Hu, K., Xu, J., Liu, R., Gong, Z., and Cai, Y.: Determining heavy metal pollution in
820 sediments from the largest impounded lake in the eastern route of China's South-to-North
821 Water Diversion Project: Ecological risks, sources, and implications for lake management, ,
822 Environ. Res., 24, 114118, https://doi.org/ 10.1016/j.envres.2022.114118, 2022.
823 Xiao, T., Boyle, D., Guha, J., Rouleau, A., Hong, Y., and Zheng, B.: Groundwater-related thallium
824 transfer processes and their impacts on the ecosystem: southwest Guizhou Province, China, ,
825 Appl. Geochem., 18(5), 675-691, https://doi.org/10.1016/S0883-2927(02)00154-3, 2003.
826 Yin, S., Wang, L., Kabwe, E., Chen, X., Yan, R., An, K., Zhang, L., and Wu, A.: Copper bioleaching
827 in China: Review and prospect, , Minerals, 8, 32, https://doi.org/10.3390/min8020032, 2018.
828 Yu, J., Liu, X., Yang, B., Li, X., Wang, P., Yuan, B., Wang, M., Liang, T., Shi, P., Li, R., Cheng, H.,
829 and Li, F.: Major influencing factors identification and probabilistic health risk assessment of
830 soil potentially toxic elements pollution in coal and metal mines across China: A systematic
831 review, , Ecotoxicol. Environ. Saf., 274, 116231,
832 https://doi.org/10.1016/j.ecoenv.2024.116231, 2024.
833 Zhang, L. -Z., Xing, S. -P., Huang, F. -Y., Xiu, W., Rensing, C., Zhao, Y., and Guo, H. M.: Metabolic
834 coupling of arsenic, carbon, nitrogen, and sulfur in high arsenic geothermal groundwater:
835 Evidence from molecular mechanisms to community ecology, , Water Res., 249, 120953,
836 https://doi.org/10.1016/j.watres.2023.120953, 2024.
837 Zhang, M. C., Chao, L. J., Yuan, L. P., Liang, W. J., Zheng, X., and Sun, K. F.: Summarize on the
838 lead and zinc ore resources of the world and China, China Mining Mag., 25, 41-45 (in Chinese
839 with English abstract), 2016a.

840 Zhang, X., Li, X., and Gao, X.: Hydrochemistry and coal mining activity induced karst water
841 quality degradation in the Niangziguan karst water system, China–, Environ. Sci. Pollut. Res.,
842 23, 6286-6299, https://doi.org/10.1007/s11356-015-5838-z, 2016b.

Supplement of

Mapping mining-affected water pollution in China: Status, patterns, risks, and implications

Ziyue Yin[1], Jian Song[2], Dianguang Liu[1], Jianfeng Wu[1,*], Yun Yang[2], Yuanyuan Sun[1], Jichun Wu[1]

[1] Key Laboratory of Surficial Geochemistry, Ministry of Education, Department of Hydrosciences, School of Earth Sciences and Engineering, Nanjing University, Nanjing 210023, China

[2] School of Earth Sciences and Engineering, Hohai University, Nanjing 211100, China

[*] Corresponding authors. Tel: +86 25 89680853; fax: +86 25 83686016

E-mail address: jfwu@nju.edu.cn (J.F. Wu)

S1 The spatial distribution of natural resources in China

The spatial distribution of coal fields shows significant regional differences, with dense concentrations in the coal-bearing areas of North and South China (Fig. S1). Among them, the southern Inner Mongolia, Shaanxi, Shanxi, and Henan provinces have the highest density of coal mines and mine production capacity. Besides, the coal resources of the junction of Anhui and Shandong provinces as well as Yunnan, Guizhou, Sichuan, and other provinces in southwest China are relatively rich (Xiao et al., 2021). Besides, the total sulfur content in different coal-bearing areas in China is shown in Fig. S2.

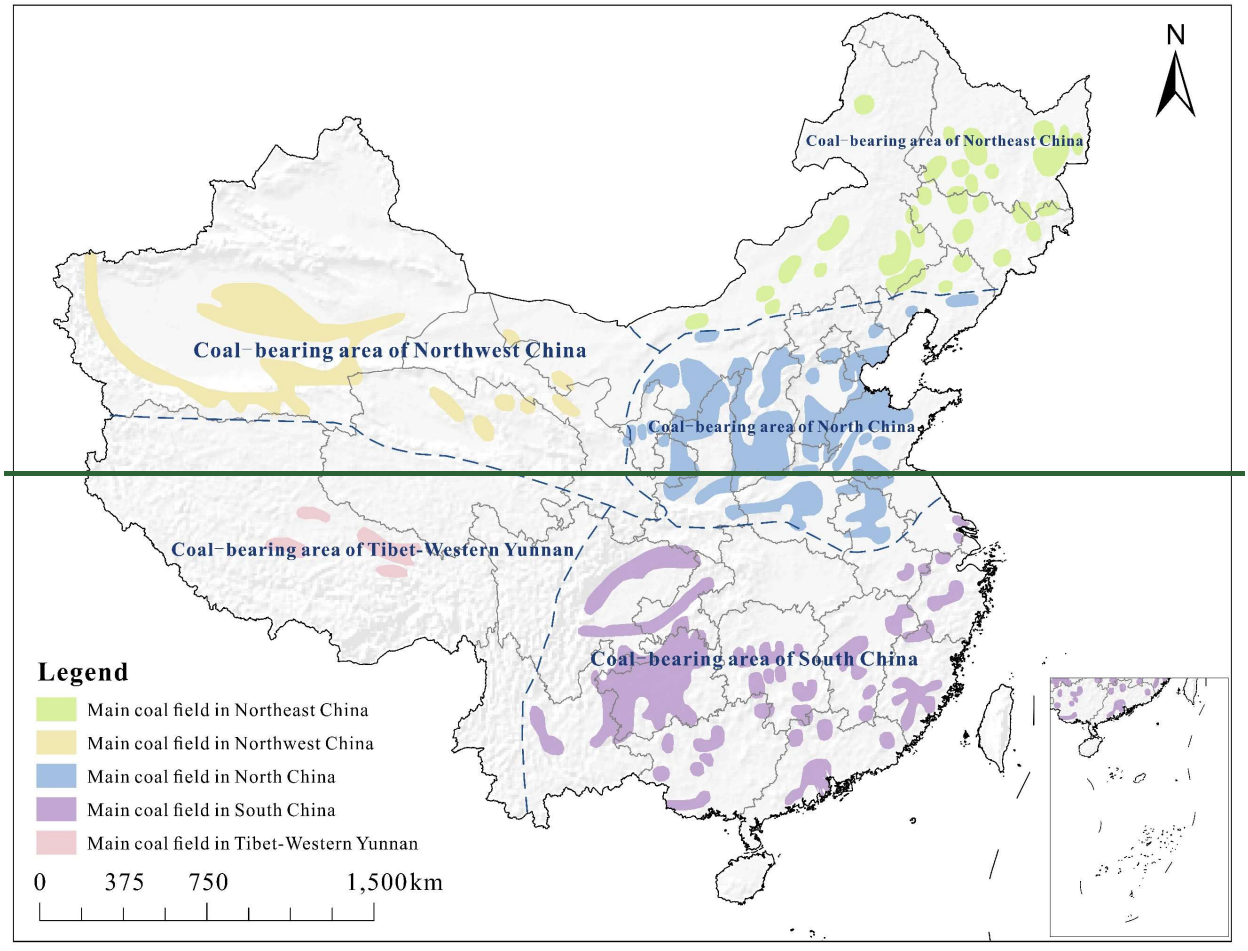

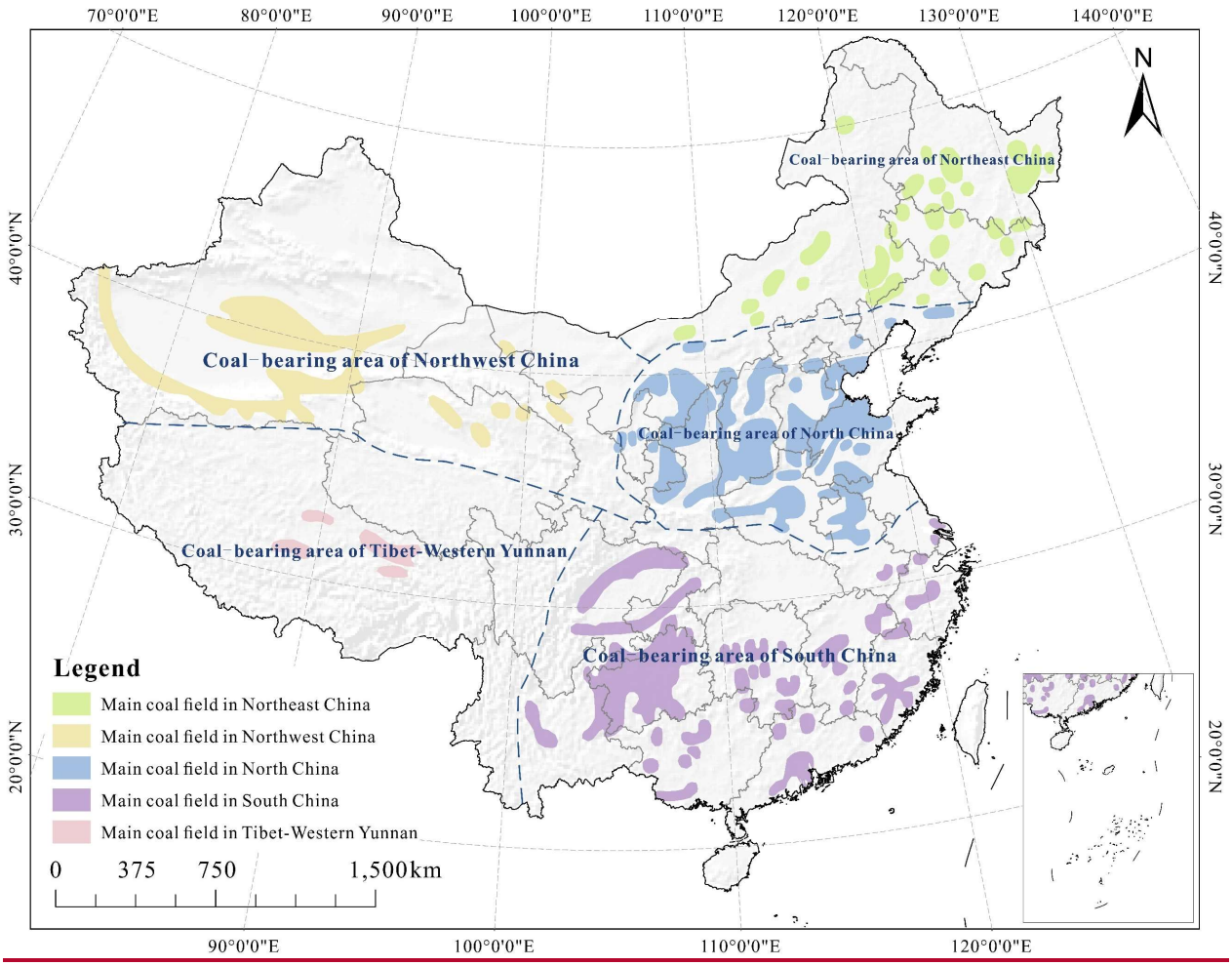

867

868 **Figure S1.** The spatial distribution of main coal-bearing areas in China (originated from China

869 National Administration of Coal Geology).

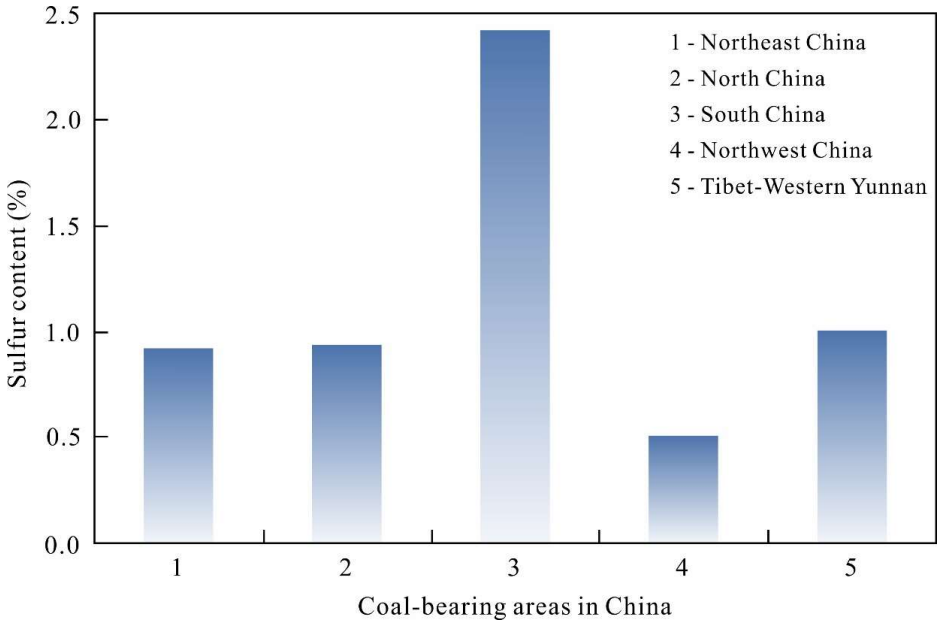

Figure S2. The total sulfur content (%) in different coal-bearing areas in China (adapted from Tang et al., 2015).

As shown in Fig. S3, China is rich in non-ferrous metal mineral resources. The predominant types are copper, lead-zinc, tin deposits, etc., mainly distributed in the provinces of Jiangxi, Yunnan, and Inner Mongolia. For example, the Dexing copper mine in Jiangxi province ranks as one of the largest copper deposits in China, while the Gejiu tin mine in Yunnan province is a world-renowned tin-producing area. Additionally, substantial precious metal mineral resources (gold and silver deposits) are predominantly located in Shandong, Henan, and Guizhou provinces. For example, the Zhaoyuan gold mine in Shandong province is a historically significant gold-producing region.

It is noteworthy that the national mineral deposit database of China developed by Li et al. (2019), covering 232 mineral resources in 27,569 deposits in 29 provinces (cities or districts), is of great importance to study the national natural resources. It can help readers catch more authoritative information, such as ore species, deposit name, location, latitude (N), longitude (E), genetic type of deposit, paragenetic mineral, associated mineral, deposit scale, ore-forming age, and mining status, enabling comprehensive analysis of China's natural resources.

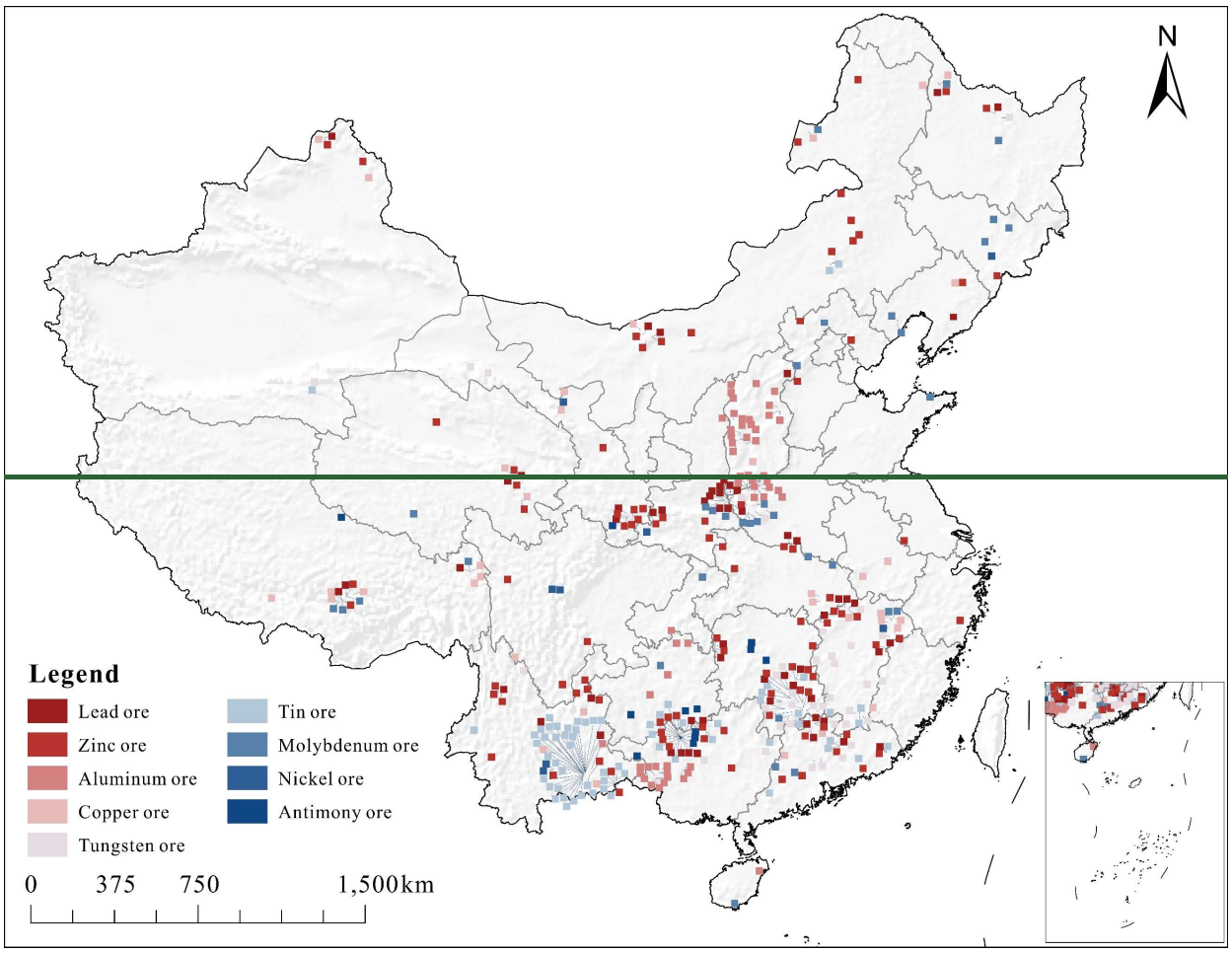
N
Legend
Lead ore
Zinc ore
Aluminum ore
Copper ore
Tungsten ore
Tin ore
Molybdenum ore
Nickel ore
Antimony ore
0
375
750
1,500km

886

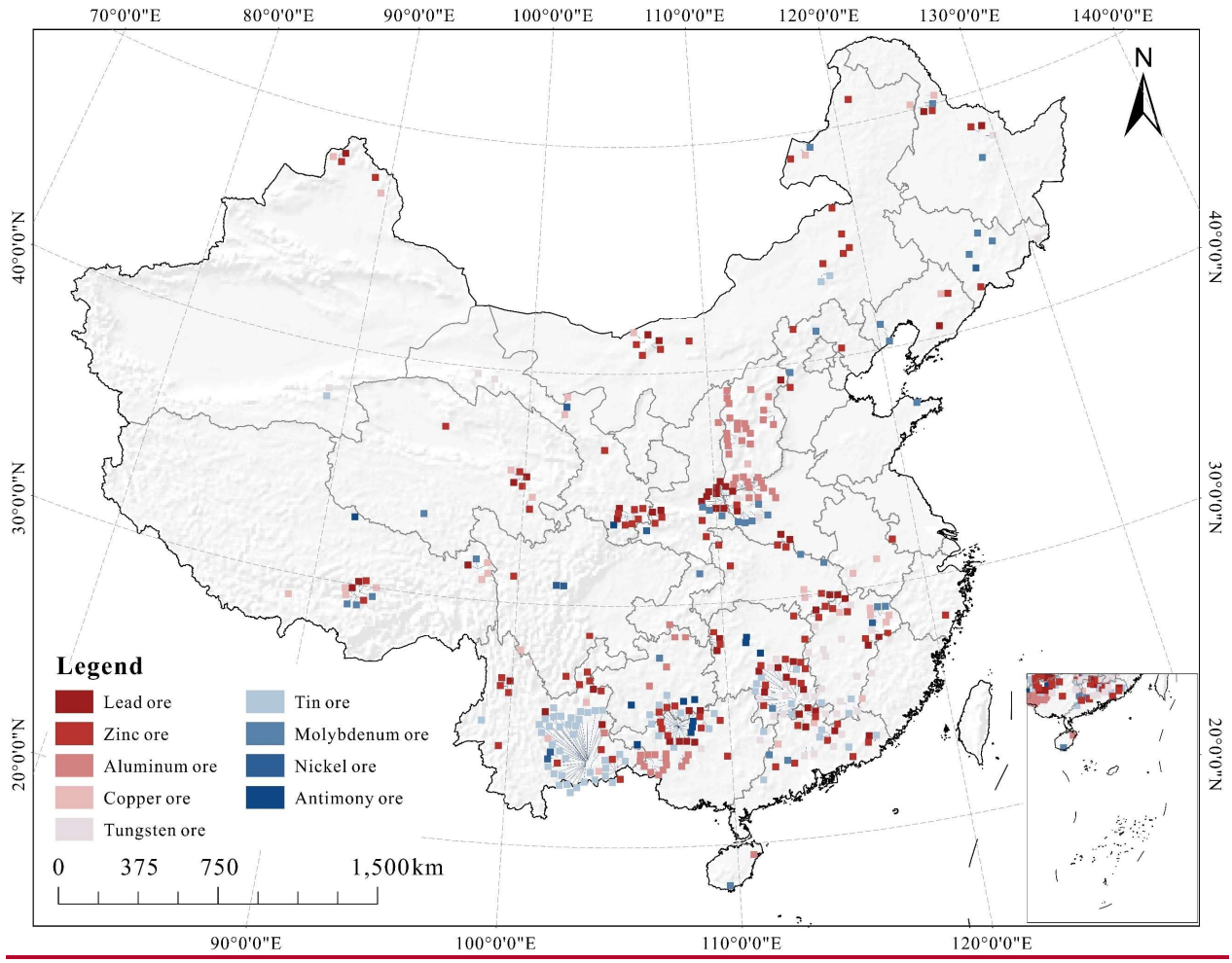

887

888 **Figure S3.** The spatial distribution of the major non-ferrous mineral resources in China (adapted

889 from China Natural Resources Atlas, China Geological Survey, 2015,

890 https://www.cgs.gov.cn/xwl/dzzl/201603/t20160309_304269.html).

S1-References

Li, C. Y., Liu, F. Y., Li, J., He, C. Z., Wang, X. C., and Wang F.: National mineral deposit database of China, Geology in China, 46(S2), 1-8 (in Chinese with English abstract), https://doi.org/10.12029/gc2019Z201, 2019.

Tang, Y. G., He, X., Cheng, A. G., Li, W. W., Deng, X. J., Wei, Q., and Li, L.: Occurrence and sedimentary control of sulfur in coals of China, J. China Coal Soc., 40(9), 1977-1988 (in Chinese with English abstract), https://doi.org/10.13225/j.cnki.jccs.2015.0434, 2015.

Xiao, W., Chen, W. Q., and Deng, X. Y.: Coupling and coordination of coal mining intensity and social-ecological resilience in China, Ecol. Indic., 131, 108167, https://doi.org/10.1016/j.ecolind.2021.108167, 2021.

S2 Database establishment

The typical mine lists are shown in Table S1 in the ESM2.xlsx document. The sources (*i.e.*, 293 research papers) of high-quality data are listed in the section of ***References*** at the end of the text.

S3 Risk assessment

Table S2. The main parameters used to assess~~for~~ the potential human health risks (*i.e.*, non-carcinogenic risks and carcinogenic risks) for adults and children in the study.~~human health risk assessment.~~

Parameter	Description	Unit	Value		Source
			Adult	Children	
IR	Ingestion rate	L/d	2.50	0.78	[1], [2]
EF	Exposure frequency	d/yr	350	350	[1], [2]
ED	Exposure duration	yr	24	6	[2]
ET	Time of contact	h/d	0.58	1.00	[3], [4]
SA	Skin surface area	cm^2	19652	6365	[1], [2]
CF	Conversion factor	L/cm^3	0.001	0.001	[2], [5]
BW	Body weight	kg	70	15	[1], [3], [4]
AT	Averaging time [a]	d	8760	2190	*ED*×365 d/yr
	Averaging time [b]	d	25550	25550	70×365 d/yr

Note: [a] averaging time used for non-carcinogenic risks (NCRs), and [b] averaging time used for carcinogenic risks (CRs), which is equal to a lifetime (70 yr in the study) ×365 d/yr. The parameter values used in the study are obtained from the following literature sources: [1] Meng et al. (2024); [2] Shi et al. (2023); [3] Tong et al. (2021); [4] Wang et al. (2021); and [5] Yuan et al. (2023).

Table S3. The values of main parameters including permeability coefficient of skin (K_p), reference dose (RfD_o), gastrointestinal digestion coefficient (ABS_{GI}), and slope factor (SF) for each element.

Parameter	K_p (cm/h)	RfD_o (mg/kg·d)	ABS_{GI} (-)	SF (kg·d/mg)	Source
Fe	0.001	0.7	0.2	-	[1], [2], [3], [4], [6]
Mn	0.001	0.024	0.04	-	[1], [2], [3], [4], [6]
Cr	0.002	0.003	0.025	0.5	[1], [3], [6], [7]
Ni	0.0002	0.02	0.04	-	[1], [2], [3], [4], [6], [7]
Cu	0.001	0.04	0.2	-	[1], [2], [3], [4], [6], [7]
Zn	0.0006	0.3	0.2	-	[1], [2], [3], [4], [5], [6]
As	0.001	0.0003	1	1.5	[1], [3], [7]
Cd	0.001	0.0005	0.05	0.38	[2], [3], [4], [6]
Pb	0.0001	0.0014	0.3	-	[1], [3], [6]

Note: The parameter values for each element are obtained from the following literature sources: [1] Meng et al. (2024); [2] Shi et al. (2023); [3] Tong et al. (2021); [4] USEPA (2002); [5] USEPA (2014); [6] Wang et al. (2021); and [7] Zheng et al. (2023).

S3-References

Meng, F., Cao, R., Zhu, X., Zhang, Y., Liu, M., Wang, J., Chen, J., and Geng, N.: A nationwide investigation on the characteristics and health risk of trace elements in surface water across China, Water Res., 250, 121076, https://doi.org/10.1016/j.watres.2023.121076, 2024.

Shi, J., Zhao, D., Ren, F., and Huang, L.: Spatiotemporal variation of soil heavy metals in China: The pollution status and risk assessment, Sci. Total Environ., 871, 161768, https://doi.org/10.1016/j.scitotenv.2023.161768, 2023.

Tong, S., Li, H., Tudi, M., Yuan, X., and Yang, L.: Comparison of characteristics, water quality and health risk assessment of trace elements in surface water and groundwater in China, Ecotox. Environ. Safe., 219, 112283, https://doi.org/10.1016/j.ecoenv.2021.112283, 2021.

USEPA: Risk-based Concentration Table, U.S. Environment Protection Agency (Washington DC), 2002.

USEPA: Human health evaluation manual, supplemental guidance: update of standard default exposure factors, Environment Protection Agency (Washington DC), 2014.

Wang, J., Liu, G., Liu, H., and Lam, P. K. S.: Multivariate statistical evaluation of dissolved trace elements and a water quality assessment in the middle reaches of Huaihe River, Anhui, China, Sci., Total Environ., 583, 421-431, https://doi.org/10.1016/j.scitotenv.2017.01.088, 2017.

Yuan, R., Li, Z., and Guo, S.: Health risks of shallow groundwater in the five basins of Shanxi, China: Geographical, geological and human activity aspects, Environ. Pollut., 316, 120524, https://doi.org/10.1016/j.envpol.2022.120524, 2023.

Zheng, X., Lu, Y., Xu, J., Geng, H., and Li, Y.: Assessment of heavy metals leachability characteristics and associated risk in typical acid mine drainage (AMD)-contaminated river sediments from North China, J. Clean. Product., 413, 137338, https://doi.org/10.1016/j.jclepro.2023.137338, 2023.

S4 Overview of mining-affected water in China

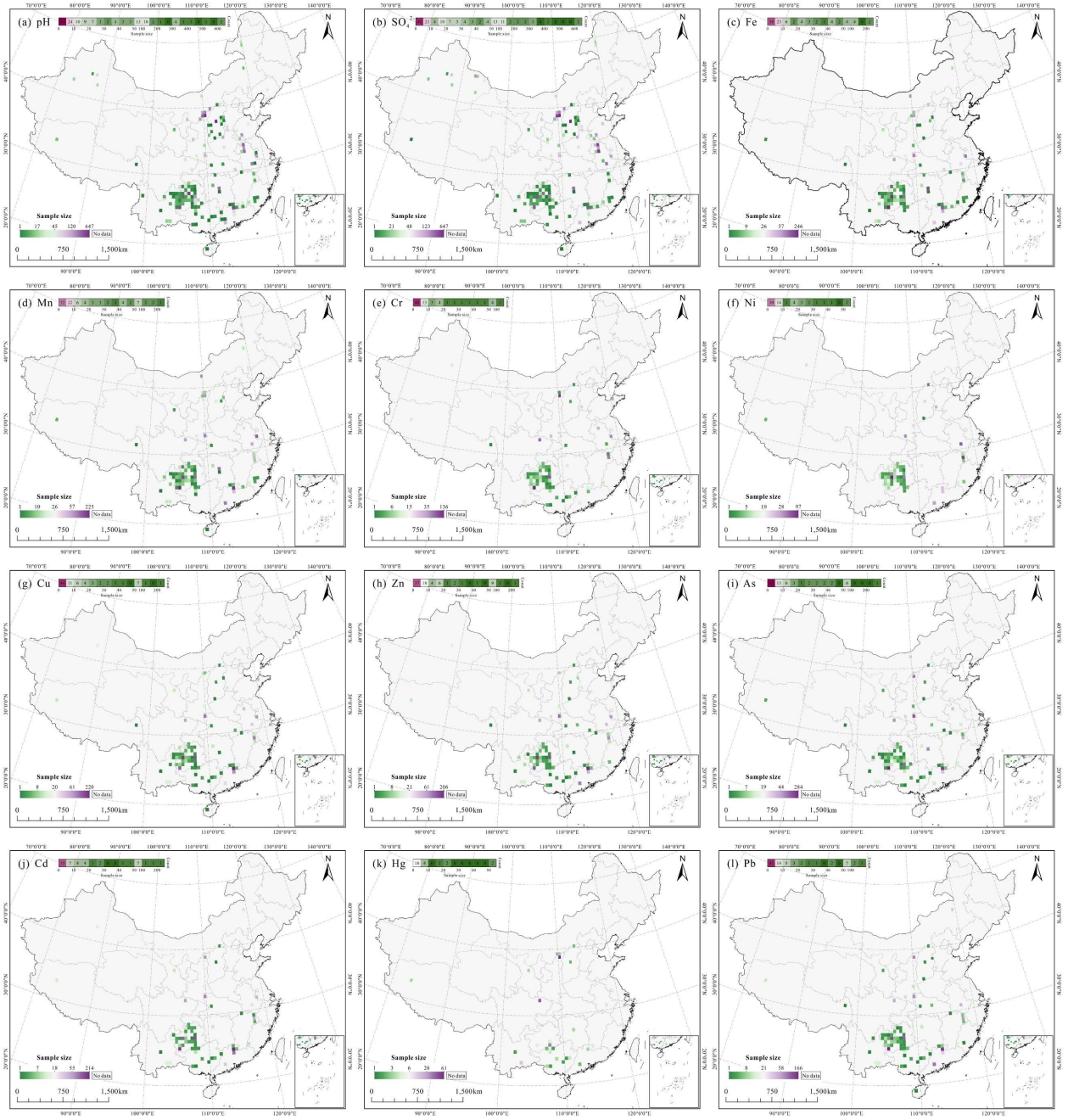

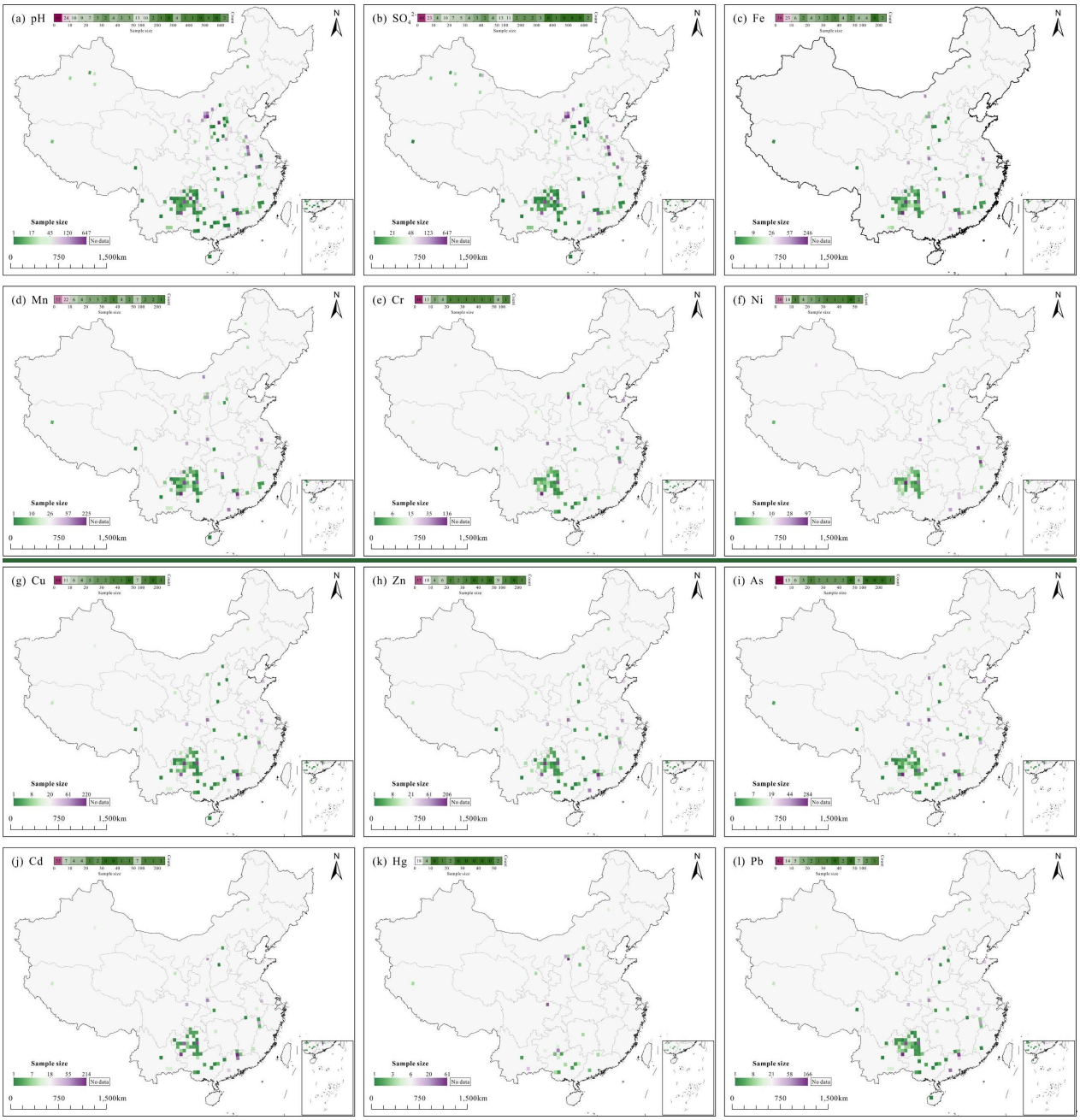

Figure S4. The spatial distribution of the sample size of (a) pH, (b) SO_4^{2-}, (c) Fe, (d) Mn, (e) Cr, (f) Ni, (g) Cu, (h) Zn, (i) As, (j) Cd, (k) Hg, and (l) Pb in mining-affected water on the 0.5° grid.

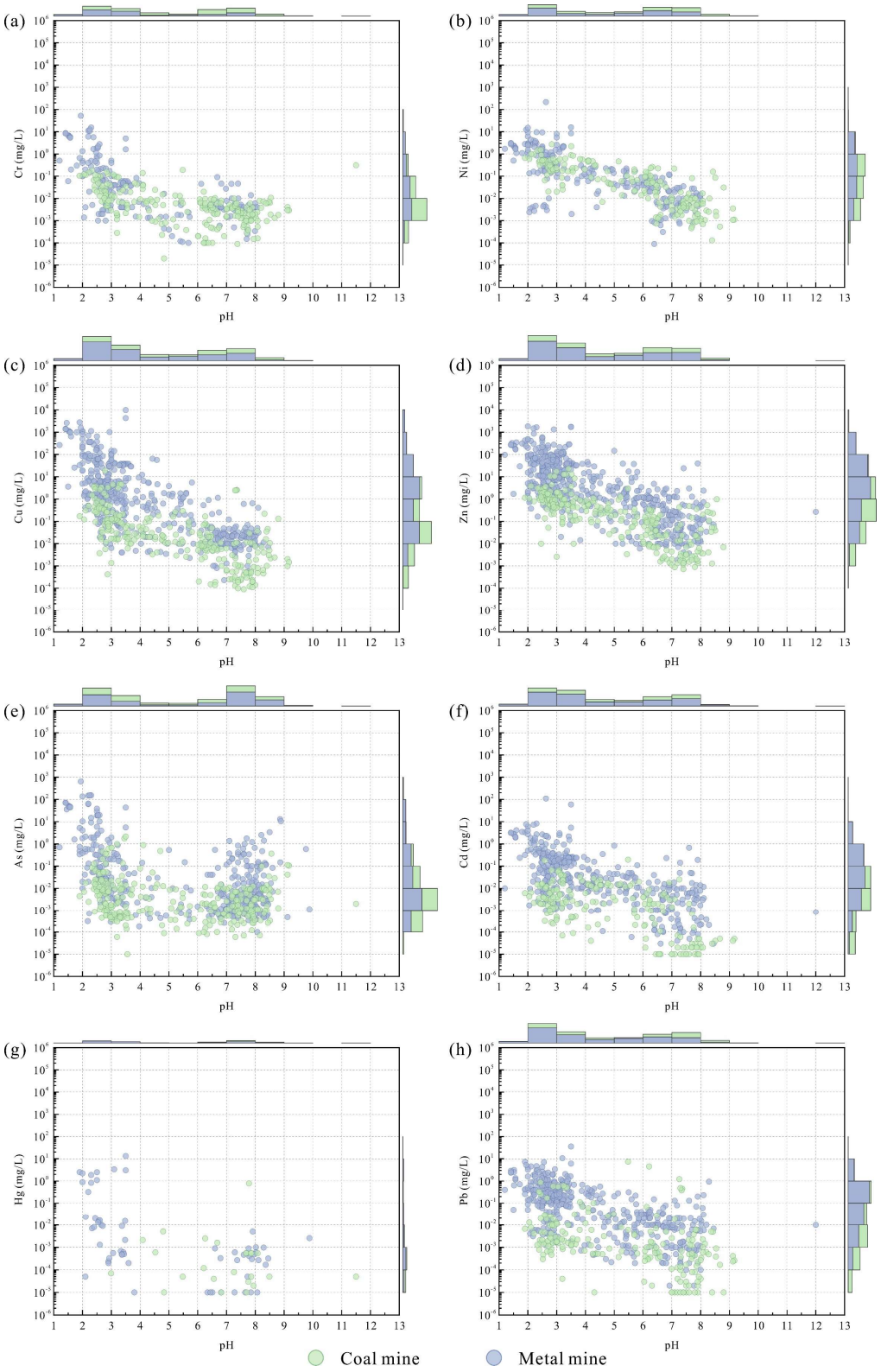

Figure S5. The ~~respective~~ relationship between pH and the respective concentrations including~~of~~ ~~pH versus~~ (a) Cr, (b) Ni, (c) Cu, (d) Zn, (e) As, (f) Cd, (g) Hg, and (h) Pb, in coal and metal mines. The binned frequency distribution of the samples is shown along the x and y axes.

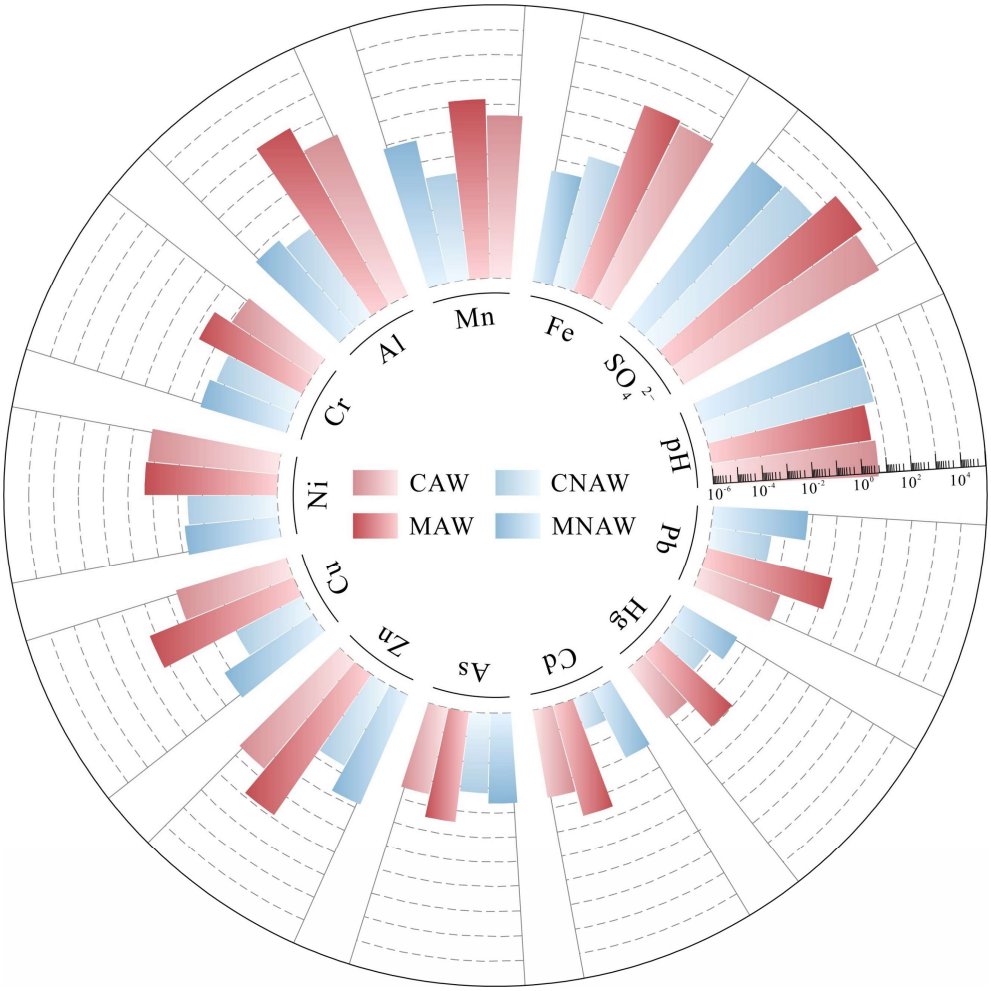

Figure S6. The median concentrations of the main species in mining-affected water from coal and metal mines (Units are mg/L except pH). CAW and MAW denote acid water from coal and metal mines; and CNAW and MNAW represent neutral/alkaline water from coal and metal mines, respectively. ~~The comparison of multi-component concentrations (mg/L, except for pH) in coal and metal mines. CAW and MAW are the acid water of coal and metal mines; and CNAW and MNAW are the neutral/alkaline water of coal and metal mines, respectively.~~

Table S4. Statistical summary (minimum, median, average, and maximum) of the main species aggregated from all samples measured in acid or non-acid mining-affected water in China (Units are mg/L except pH)~~The statistics of mining-affected water in China (Units are mg/L except pH)~~.

Item	Acid mining-affected water						Non-acid mining-affected water					
	Coal mine			Metal mine			Coal mine			Metal mine		
	Min	Median	Max	Min	Median	Max	Min	Median	Max	Min	Median	Max
pH	1.90	4.50	6.50	1.20	3.10	6.50	6.51	7.82	11.51	6.51	7.70	12.60
Na^+	0.02	18.55	1305.33	0.00	13.72	1613	0.23	234.75	7594.32	0.55	27.30	9371
K^+	0.04	3.50	37.00	0.00	2.99	172.00	0.00	2.84	164.42	0.20	3.80	419.00
Ca^{2+}	0.83	277.84	987.97	1.70	310.00	893.00	0.00	61.38	689.10	0.01	80.20	4841.70
Mg^{2+}	0.01	59.60	1665	0.10	89.52	10992	0.00	19.09	485.44	0.10	18.54	12752
Cl^-	0.06	2.51	477.24	0.00	9.20	3097.40	0.00	65.20	6462.75	0.35	19.00	26265
SO_4^{2-}	15.00	1381.59	17870	0.56	2982	181000	0.01	193.51	10110	0.09	157.41	52915
HCO_3^-	0.00	0.00	532.96	0.00	15.51	769.00	0.00	280.60	4976.61	0.62	169.50	2482
NO_3^-	0.00	0.55	143.65	0.00	1.45	735.60	0.00	3.00	356.97	0.00	11.00	1774.95
F^-	0.00	0.67	238.34	0.01	0.80	67.40	0.00	0.91	11.65	0.01	0.72	100.00

Item	Acid mining-affected water						Non-acid mining-affected water					
	Coal mine			Metal mine			Coal mine			Metal mine		
	Min	Median	Max	Min	Median	Max	Min	Median	Max	Min	Median	Max
Fe	0.00	77.41	2331.86	0.00	113.77	65250	0.00	0.25	205.00	0.00	0.03	495.43
Mn	0.00	3.50	88.40	0.00	15.82	5050	0.00	0.02	5.02	0.00	0.76	200000
Al	0.00	12.87	440.00	0.00	152.00	13679	0.00	0.02	25.00	0.00	0.05	2.09
Cr	0.00	0.0080	0.19	0.00	0.0500	52.27	0.00	0.0022	0.31	0.00	0.0041	0.09
Ni	0.0007	0.1796	2.73	0.00	0.2142	216.00	0.0001	0.0040	0.23	0.00	0.0059	0.12
Cu	0.00	0.0431	18.50	0.00	1.7325	9777.77	0.0001	0.0010	2.56	0.00	0.0180	1.14
Zn	0.0026	0.4211	23.00	0.00	7.2000	1834	0.00	0.0048	0.98	0.00	0.0617	39.30
As	0.00	0.0034	2.16	0.00	0.0281	641.70	0.0001	0.0016	0.37	0.0001	0.0040	13.00
Cd	0.00	0.0036	0.19	0.00	0.0383	110.00	0.00	0.0000	0.03	0.00	0.0010	0.67
Hg	0.00	0.0004	0.01	0.00	0.0090	13.36	0.00	0.0001	0.78	0.00	0.0003	0.01
Pb	0.00	0.0023	7.43	0.00	0.1498	35.68	0.00	0.0003	1.22	0.00	0.0064	0.94

960

Non-parametric tests do not rely on assumptions about the distribution of the data and are suitable for non-normally distributed datasets or those containing outliers. These methods statistically compare central tendencies, typically represented by medians, rather than means. The result of the Mann-Whitney U-test ($p < 0.05$) shows a statistically significant difference in the critical parameters (except Fe) of mining-affected water based on the different mine types (coal mine vs. metal mine), indicating the differences caused by geological factors, mining practices, surrounding environment, etc. Besides, Fig. S7 shows the Spearman correlation coefficients between the hydrochemical compositions in the mining-affected water. It can be seen that strong negative correlations are observed between pH and SO_4^{2-}, Fe, Mn, Al, and heavy metals, while positive correlations are observed between SO_4^{2-} and metal components, implying that the spatial consistency of acid water, high sulfate, high Fe and Mn, and high heavy metal mining-affected water.

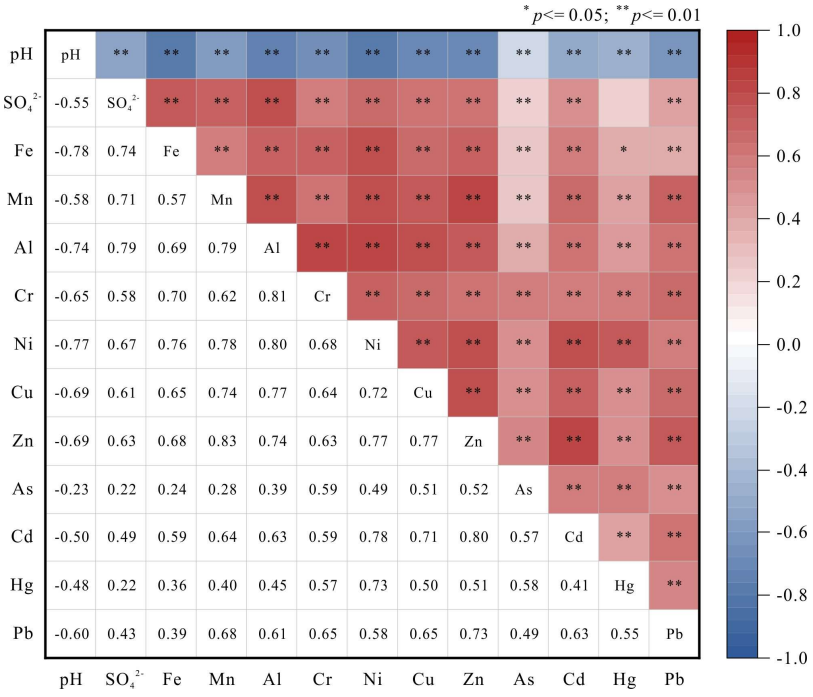

Figure S7. The Spearman correlation coefficient between the hydrochemical compositions in the mining-affected water (* is $p \leqslant 0.05$ and ** is $p \leqslant 0.01$).

S5 Spatial patterns of mining-affected water pollution in China

Table S5. The categories of the Environmental Quality Standards for Surface Water (GB 3838-2002).

Item	Class I	Class II	Class III	Class IV	Class V
pH			6.0 – 9.0		
SO_4	-	-	-	-	-
Fe	-	-	-	-	-
Mn	-	-	-	-	-
Cr	0.01	0.05	0.05	0.05	0.1
Ni	-	-	-	-	-
Cu	0.01	1.0	1.0	1.0	1.0
Zn	0.05	1.0	1.0	2.0	2.0
As	0.05	0.05	0.05	0.1	0.1
Cd	0.001	0.005	0.005	0.005	0.01
Hg	0.00005	0.00005	0.0001	0.001	0.001
Pb	0.01	0.01	0.05	0.05	0.1

Table S6. The categories of the Standard for Groundwater Quality (GB/T14848-2017).

Item	Class I	Class II	Class III	Class IV	Class V
pH		6.5 – 8.5		5.5 – 6.5 and 8.5 – 9.0	< 5.5 and > 9.0
SO4	50	150	250	350	> 350
Fe	0.1	0.2	0.3	2.0	> 2.0
Mn	0.05	0.05	0.1	1.5	> 1.5
Cr	0.005	0.01	0.05	0.1	> 0.1
Ni	0.002	0.002	0.02	0.1	> 0.1
Cu	0.01	0.05	1.0	1.5	> 1.5
Zn	0.05	0.5	1.0	5.0	> 5.0
As	0.001	0.001	0.01	0.05	> 0.05
Cd	0.0001	0.001	0.005	0.01	> 0.01
Hg	0.0001	0.0001	0.001	0.002	> 0.002
Pb	0.005	0.005	0.01	0.1	> 0.1

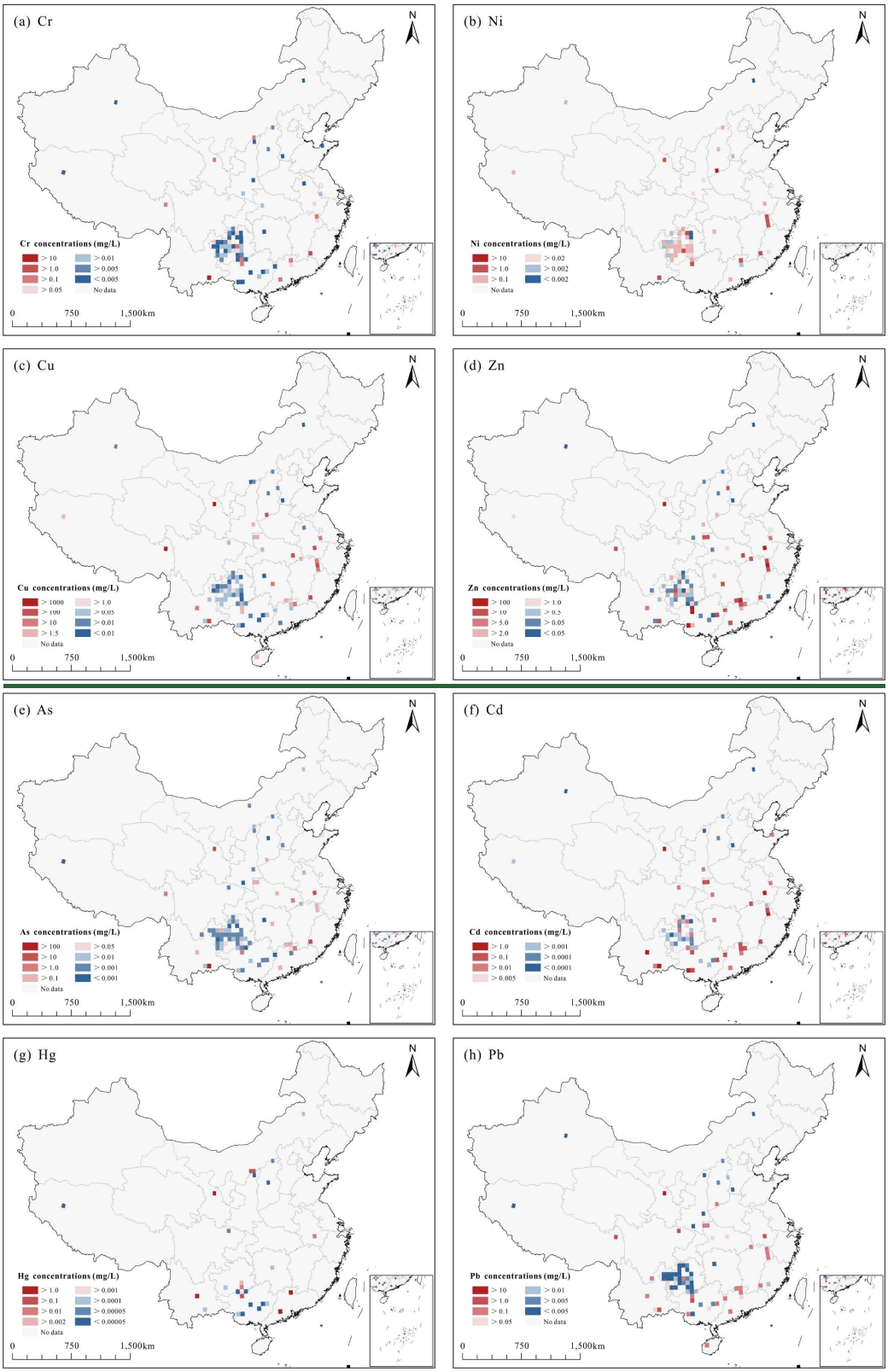
(a) Cr
Cr concentrations (mg/L)
> 10
> 1.0
> 0.1
> 0.05
> 0.01
> 0.005
< 0.005
No data
(b) Ni
Ni concentrations (mg/L)
> 10
> 1.0
> 0.1
> 0.02
> 0.002
< 0.002
No data
(c) Cu
Cu concentrations (mg/L)
> 1000
> 100
> 10
> 1.5
> 1.0
> 0.05
> 0.01
< 0.01
No data
(d) Zn
Zn concentrations (mg/L)
> 100
> 10
> 5.0
> 2.0
> 1.0
> 0.5
> 0.05
< 0.05
No data
(e) As
As concentrations (mg/L)
> 100
> 10
> 1.0
> 0.1
> 0.05
> 0.01
> 0.001
< 0.001
No data
(f) Cd
Cd concentrations (mg/L)
> 1.0
> 0.1
> 0.01
> 0.005
> 0.001
> 0.0001
< 0.0001
No data
(g) Hg
Hg concentrations (mg/L)
> 1.0
> 0.1
> 0.01
> 0.002
> 0.001
> 0.0001
> 0.00005
< 0.00005
No data
(h) Pb
Pb concentrations (mg/L)
> 10
> 1.0
> 0.1
> 0.05
> 0.01
> 0.005
< 0.005
No data
N
0
750
1,500km

981

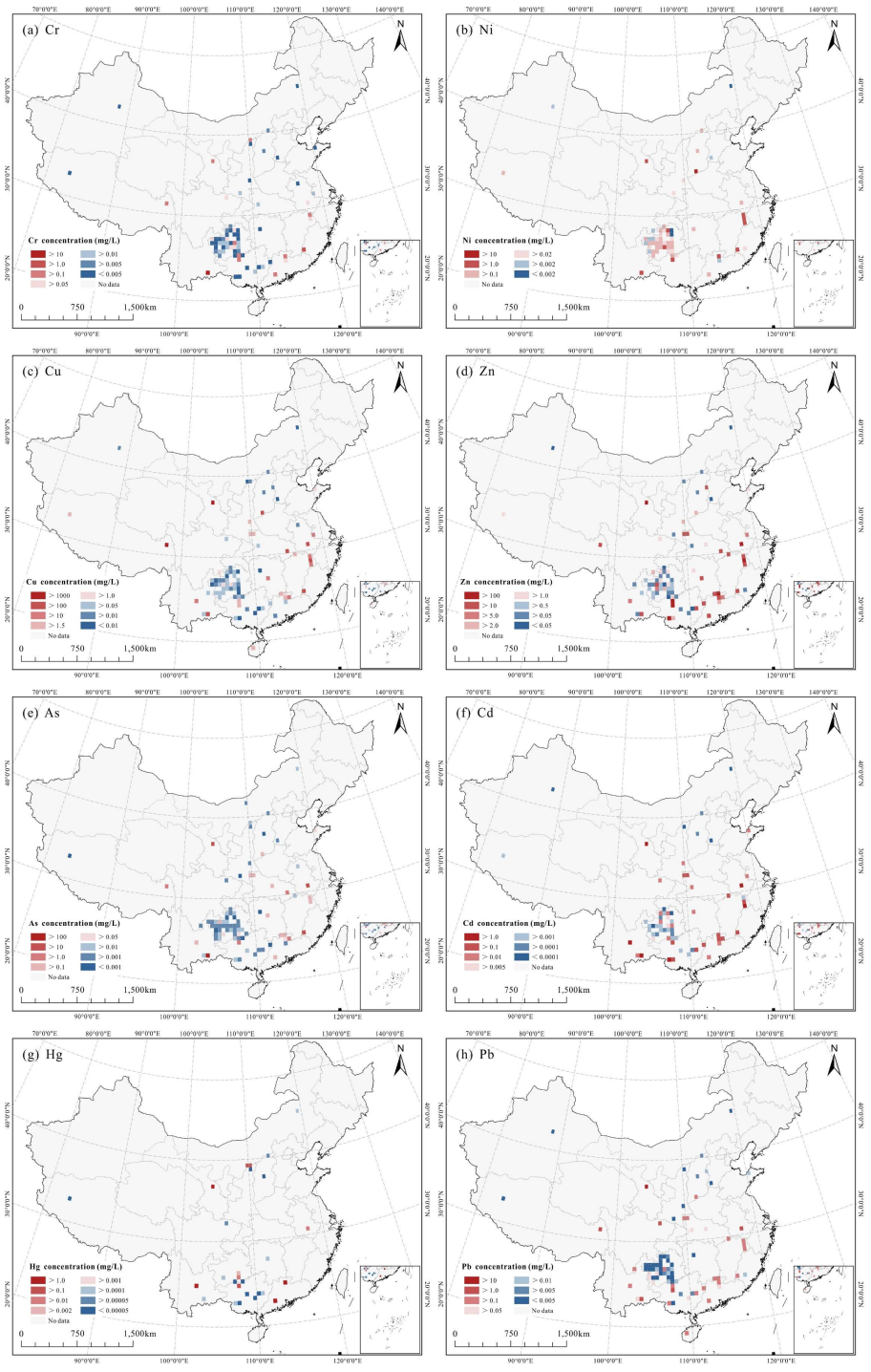

982

983 **Figure S8.** The spatial distribution of mean concentration of individual components (mg/L)

984 showing respective (a) Cr, (b) Ni, (c) Cu, (d) Zn, (e) As, (f) Cd, (g) Hg, and (h) Pb in mining-

985 affected water on the 0.5° grid. The classification thresholds for the main components are based on

986 the distribution of all collected data, as well as regulatory benchmarks from GB 3838-2002 and

987 GB/T 14848-2017 in China.

S6 Risks of mining-affected water in China

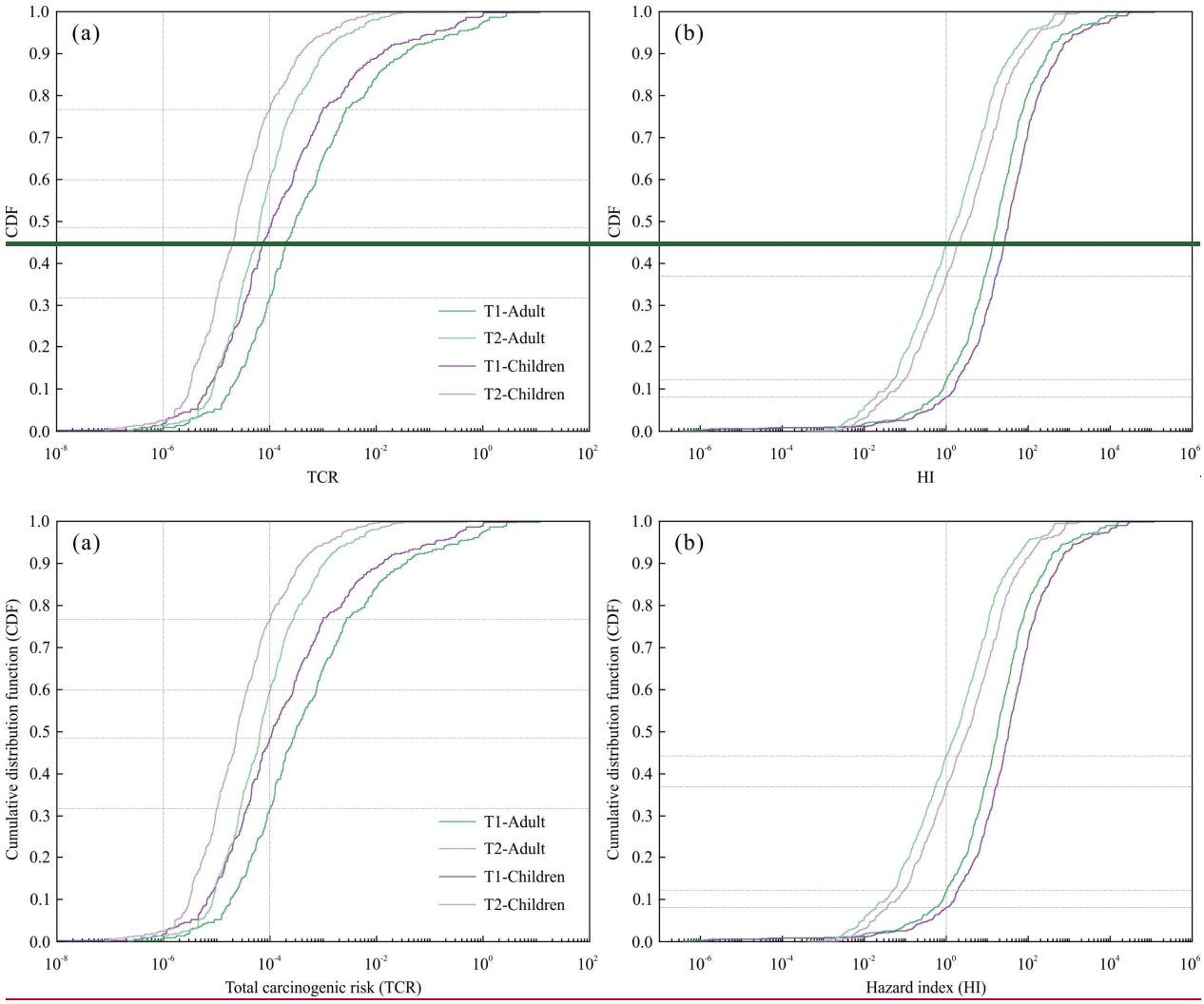

Figure S9. The cumulative distribution function (CDF) of (a) total carcinogenic risk (TCR) and (b) hazard index (HI) in mining-affected water. TCR > 10^{-4} signifies a significant risk to human health, while 10^{-6} ≤ TCR ≤ 10^{-4} represents an acceptable risk level. Similarly, HI > 1 suggests potential adverse health effects, whereas HI < 1 indicates no non-carcinogenic risk (NCR). T1 category includes mine drainage, mine water, and leachate water, while T2 category indicates mining-affected surface water and groundwater.

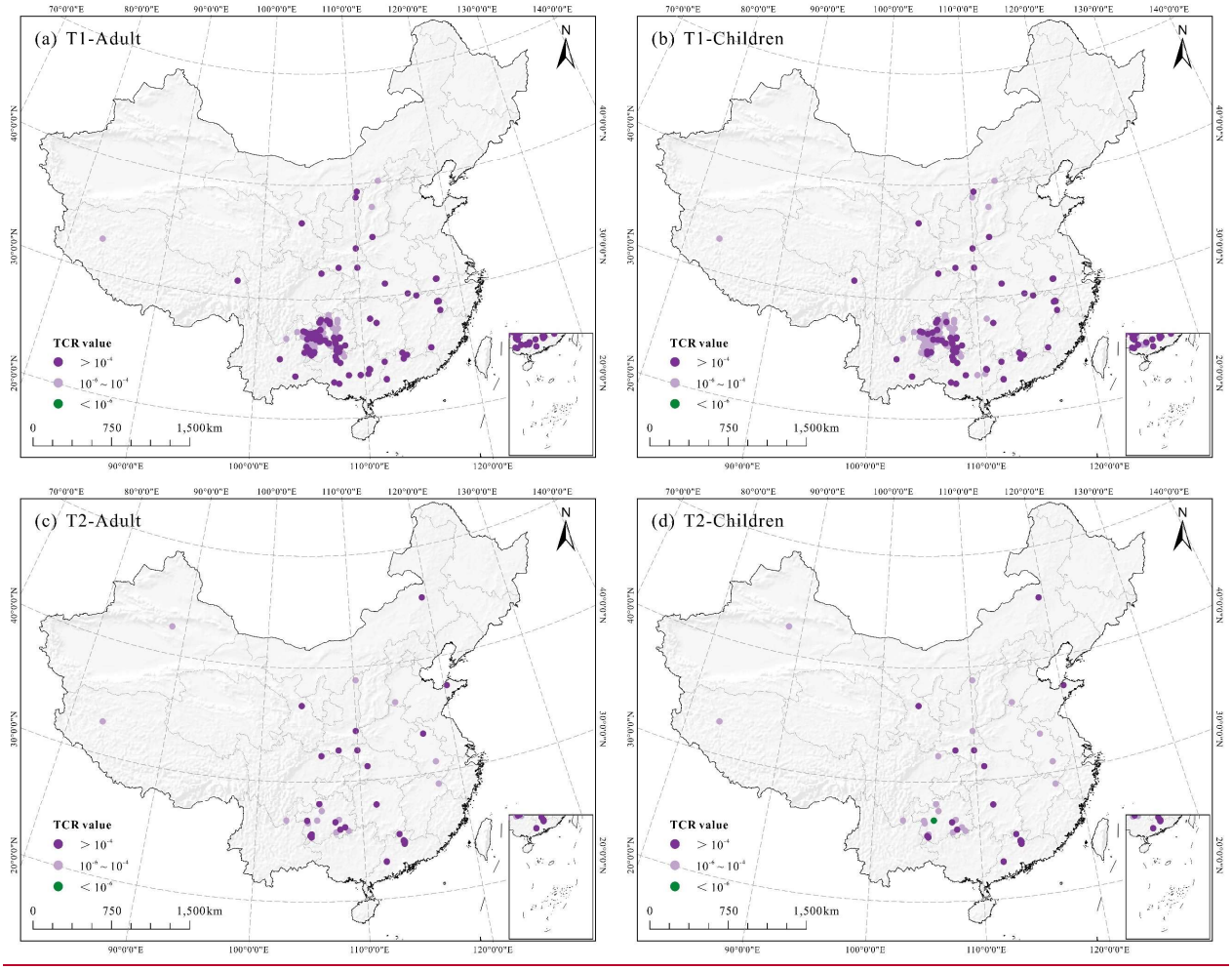
(a) T1-Adult
(b) T1-Children
(c) T2-Adult
(d) T2-Children
TCR value
$> 10^{-4}$
$10^{-6} \sim 10^{-4}$
$< 10^{-6}$
0 750 1,500km
N

997

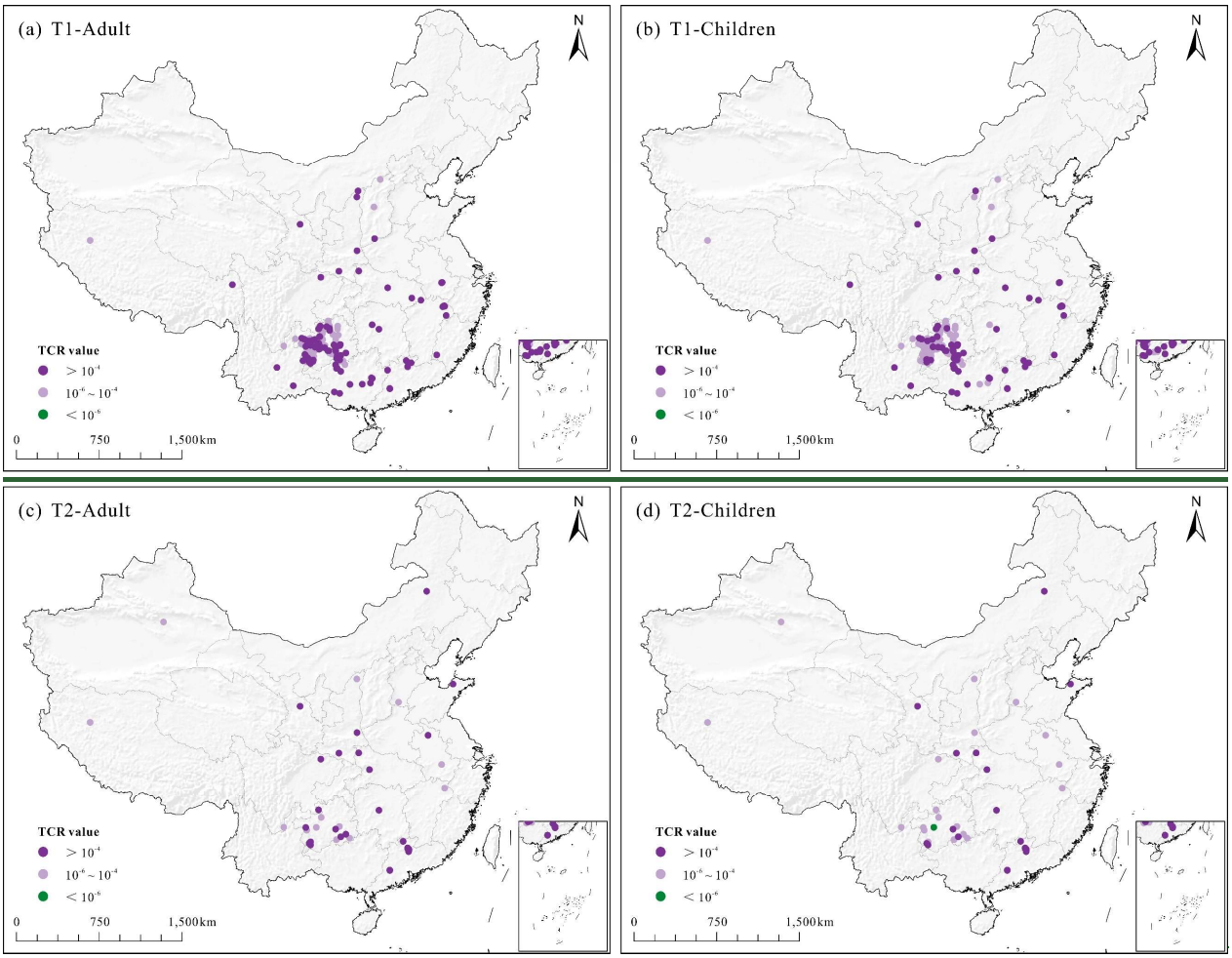

Figure S10. The spatial distribution of total carcinogenic risk (TCR)~~TCR~~ levels for (a) T1-Adult, (b) T1-Children, (c) T2-Adult, and (d) T2-Children. TCR > 10^{-4} signifies a significant risk to human health, while $10^{-6} \leq$ TCR $\leq 10^{-4}$ represents an acceptable risk level. T1 category includes mine drainage, mine water, and leachate water, while T2 category indicates mining-affected surface water and groundwater.

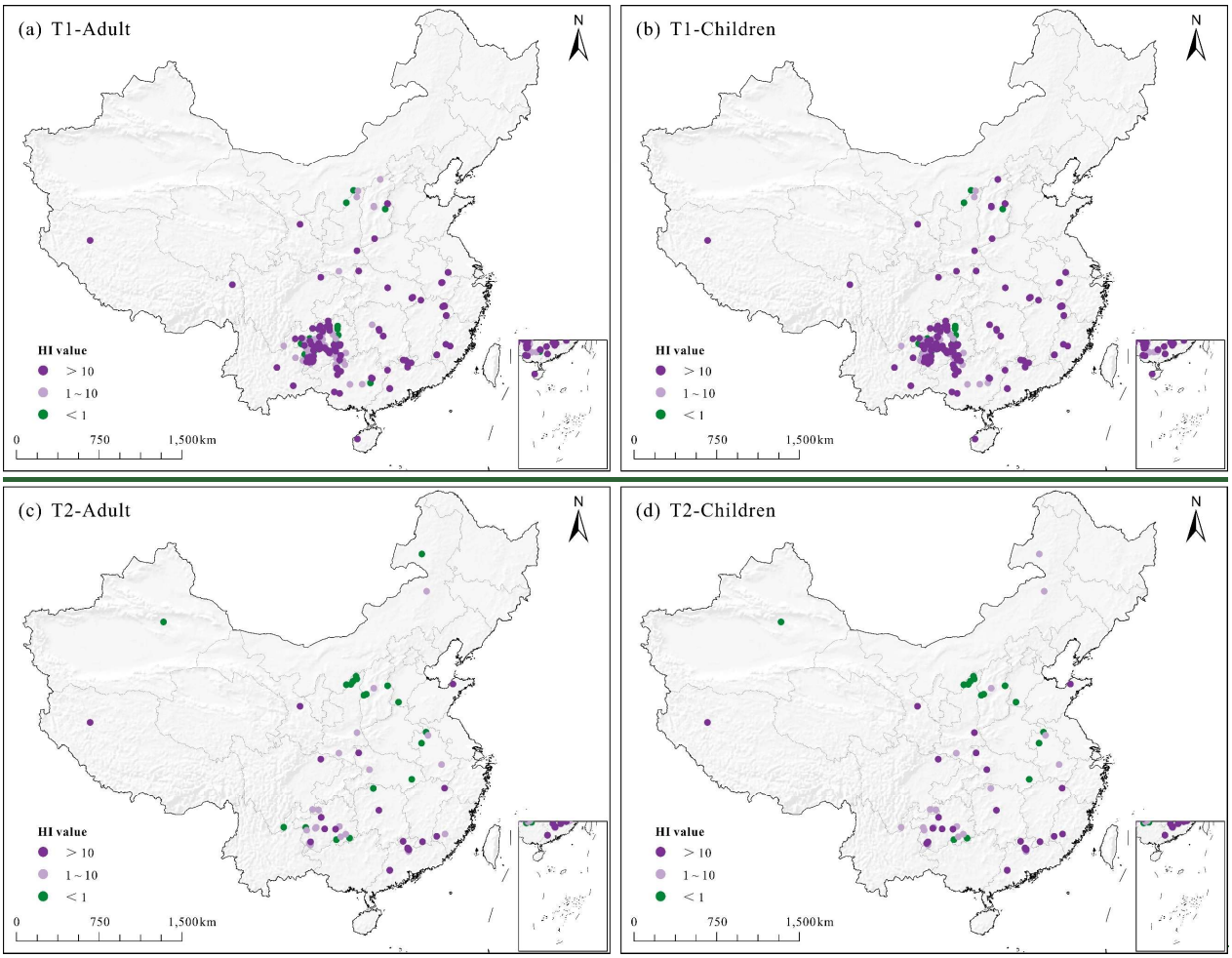
(a) T1-Adult
(b) T1-Children
(c) T2-Adult
(d) T2-Children
N
HI value
＞10
1～10
＜1
0
750
1,500km

1004

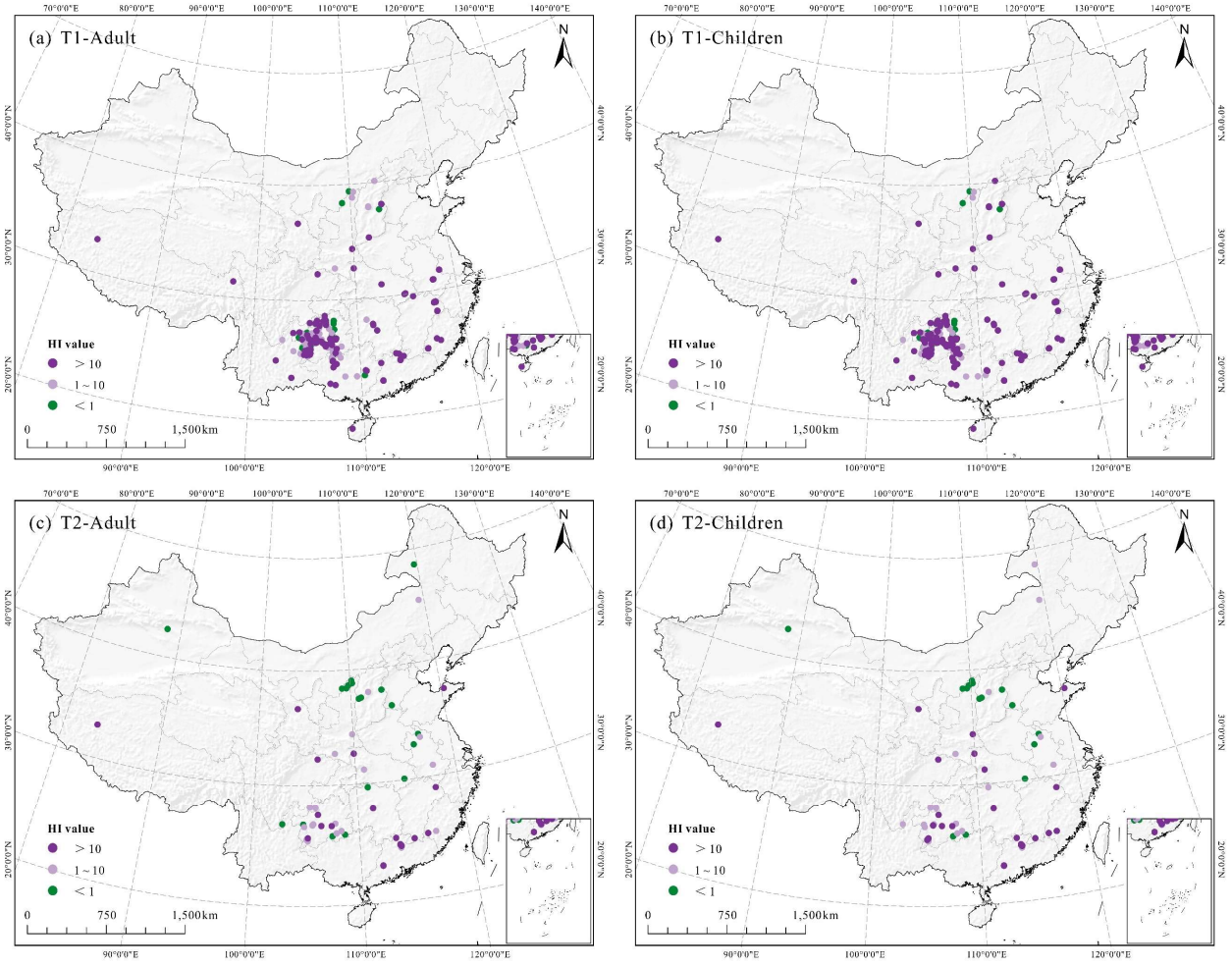

Figure S11. The spatial distribution of hazard index (HI)~~HI~~ levels for (a) T1-Adult, (b) T1-Children, (c) T2-Adult, and (d) T2-Children. HI > 1 suggests potential adverse health effects, whereas HI < 1 indicates no non-carcinogenic risk (NCR). T1 category includes mine drainage, mine water, and leachate water, while T2 category indicates mining-affected surface water and groundwater.